

Review

Sensing Methods for Hazardous Phenolic Compounds Based on Graphene and Conducting Polymers-Based Materials

Hazwani Suhaila Hashim ¹, Yap Wing Fen ^{1,2,*}, Nur Alia Sheh Omar ^{1,2} and Nurul Illya Muhamad Fauzi ²

¹ Department of Physics, Faculty of Science, Universiti Putra Malaysia, Serdang 43400, Selangor, Malaysia; hazwanisuhaila@gmail.com (H.S.H.); nuralia.upm@gmail.com (N.A.S.O.)

² Functional Devices Laboratory, Institute of Advanced Technology, Universiti Putra Malaysia, Serdang 43400, Selangor, Malaysia; illyafauzi97@gmail.com

* Correspondence: yapwingfen@upm.edu.my

Abstract: It has been known for years that the phenolic compounds are able to exert harmful effects toward living organisms including humans due to their high toxicity. Living organisms were exposed to these phenolic compounds as they were released into the environment as waste products from several fast-growing industries. In this regard, tremendous efforts have been made by researchers to develop sensing methods for the detection of these phenolic compounds. Graphene and conducting polymers-based materials have arisen as a high potential sensing layer to improve the performance of the developed sensors. Henceforth, this paper reviews the existing investigations on graphene and conducting polymer-based materials incorporated with various sensors that aimed to detect hazardous phenolic compounds, i.e., phenol, 2-chlorophenol, 2,4-dichlorophenol, 2,4,6-trichlorophenol, pentachlorophenol, 2-nitrophenol, 4-nitrophenol, 2,4-dinitrophenol, and 2,4-dimethylphenol. The whole picture and up-to-date information on the graphene and conducting polymers-based sensors are arranged in systematic chronological order to provide a clearer insight in this research area. The future perspectives of this study are also included, and the development of sensing methods for hazardous phenolic compounds using graphene and conducting polymers-based materials is expected to grow more in the future.

Keywords: conducting polymers; graphene-based materials; hazardous phenolic compounds; sensors; surface plasmon resonance



Citation: Hashim, H.S.; Fen, Y.W.; Omar, N.A.S.; Fauzi, N.I.M. Sensing Methods for Hazardous Phenolic Compounds Based on Graphene and Conducting Polymers-Based Materials. *Chemosensors* **2021**, *9*, 291. <https://doi.org/10.3390/chemosensors9100291>

Academic Editors: Maria Grzeszczuk and Barbara Palys

Received: 18 August 2021

Accepted: 28 September 2021

Published: 14 October 2021

Publisher's Note: MDPI stays neutral with regard to jurisdictional claims in published maps and institutional affiliations.



Copyright: © 2021 by the authors. Licensee MDPI, Basel, Switzerland. This article is an open access article distributed under the terms and conditions of the Creative Commons Attribution (CC BY) license (<https://creativecommons.org/licenses/by/4.0/>).

1. Introduction

Phenolic compounds play an important role in the rapid development of the industrial sector. It has been used as the raw materials in the production and manufacturing of resins, plastics, germicides, pharmaceutical, textiles, dyes, and petrochemical products [1–5]. Then, they are released into the environment as by-products contaminants. Any consumption of liquids with a high concentration of phenolic compounds can lead to difficulty in walking. In fact, excessive exposure to high levels of phenolic compounds can even cause damage to the heart, kidneys, and liver [6–9].

Thus, the removal of the phenolic compounds from water and wastewater has become a hot topic among scientists considering the high toxicity and persistency of the phenolic compounds [10]. Thereby, many methods have been introduced to eliminate the phenolic compounds from the contaminated places including distillation, adsorption, incineration, solvent extraction, chemical oxidation, and membrane separation [11]. Consequently, a lot of materials have been used during the removal of phenolic compounds to improve the effectiveness of the processes.

Among them, graphene-based materials are one of the most remarkable materials due to their outstanding properties of strong adsorption capacity, excellent electrical conductivity, and optical properties [12–14]. Graphene is a two-dimensional nanostructure that consists of a single layer of sp² hybridized carbon atoms arranged in a honeycomb-like lattice [15–17]. A three-dimensional graphite will be formed through the stacking of graphene

sheets by weak van der Waals forces [18]. Graphene oxide is a monolayer of graphite oxide containing both sp^2 and sp^3 carbon atoms; meanwhile, reduced graphene oxide can be obtained by the reduction process of graphene oxide via chemical or electrochemical methods [19,20]. The electrochemical behavior of the reduced graphene oxide is way better compared to graphene oxide with higher conductivity [21]. Lastly, graphene quantum dots are the zero-dimensional monolayer graphene sheet with a size of nanometers [22]. Graphene quantum dots are unique, since they carry both the properties of graphene and quantum dots. These graphene-based materials were able to remove phenolic compounds with a high removal efficiency of more than 90% [23,24].

Alongside graphene-based materials, conducting polymers-based materials also have appeared as a high-potential material in the removal of phenolic compounds [25,26]. Conducting polymers are well known for their excellent optical, electric, electrical, and magnetic properties [27–30]. Conducting polymers also possess great electrocatalytic properties and rapid electron transfer ability owing to their conducting nature [31,32]. Conducting polymers also have been widely used in various applications such as batteries [33], electrochromic devices [34], actuators [35,36], and supercapacitors [37].

Apart from being used in the removal of phenolic compounds, graphene and conducting polymers-based materials have shown a great potential as sensing materials [38–40]. They have been extensively fabricated in sensors for the detection of phenolic compounds that able to detect the target analytes down to the range of femtomolars.

Graphene-based materials are highly known as an ideal material in sensing application as they have a large surface area, exceptional electron mobility, great mechanical properties, and excellent electrochemical activity [41,42]. Their easy availability, low cost, and light weight are also reasons behind their popularity [43]. Unlike carbon nanotubes, graphene-based materials do not contain metallic impurities and can be easily fabricated into complex sensors through traditional microfabrication approaches [44]. Furthermore, the electrical conductivity of graphene-based materials is about 60 times higher compared to carbon nanotubes [45].

As for conducting polymers, they have been widely utilized in the field of sensors due to the ability to reversely change their electrical and optical properties through doping and undoping processes [46–48]. These conducting polymers also possess several advantages such as cost-effectiveness, excellent environmental stability, good biocompatibility, and sensitive to small perturbations, which are advantages in designing sensors [49,50].

Electrochemical sensors are the most commonly developed sensor for the detection of phenolic compounds that may be due to their advantages such as being easy to use, cost-effectiveness, measuring in real time, good sensitivity, and easy miniaturization [51–57]. Next, sample preparation by extraction methods coupled with chromatographic analysis have emerged due to its simplicity, rapidity, and ability to retain high recoveries [58]. The main purposes of the extraction methods are for trace enrichment and sample clean-up from co-existing species. In addition, optical sensors also have become a favorable sensor among researchers for the detection of phenolic compounds. This is owing to their beneficial features such as simple, rapid detection, high efficiency, and great sensitivity and selectivity [59,60].

Henceforth, this paper firstly reviews the studies of graphene-based materials incorporated with various sensors focusing on the detection of phenol (Ph), 2-chlorophenol (2-CP), 2,4-dichlorophenol (2,4-DCP), 2,4,6-trichlorophenol (2,4,6-TCP), pentachlorophenol (PCP), 2-nitrophenol (2-NP), 4-nitrophenol (4-NP), 2,4-dinitrophenol (2,4-DNP), and 2,4-dimethylphenol (2,4-DMP) that are classified as the hazardous substances by the United States Environmental Protection Agency [61,62]. It is followed by conducting polymers-based sensors. The reviews are categorized according to the type of sensors (electrochemical sensors, extraction methods with chromatographic analysis, and optical sensors) followed by the materials used. Next, an overview of the graphene and conducting polymers-based composite materials in the development of sensors for the hazardous phenolic compounds is also discussed. The schematic representation of the materials and sensing methods discussed in this paper is as illustrated in Figure 1.

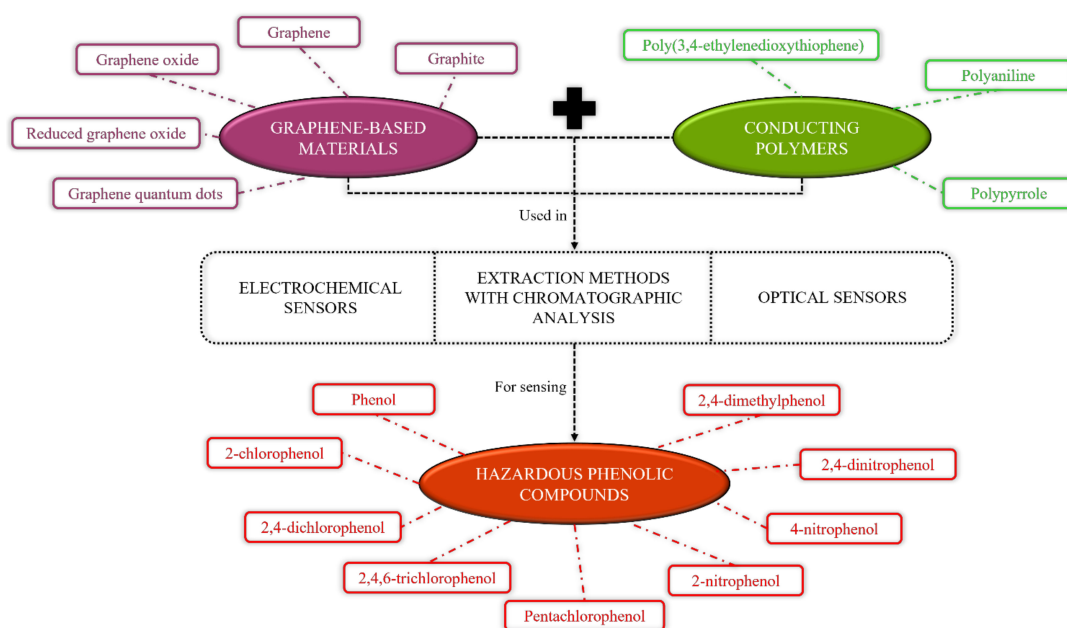


Figure 1. Schematic preparation of the materials and sensing methods discussed in this paper.

2. Graphene-Based Materials Incorporated with Various Sensors for the Detection of Hazardous Phenolic Compounds

2.1. Electrochemical Sensors

2.1.1. Graphite

Graphite has been receiving a lot of attention from researchers in the field of electrochemical sensors especially as a working electrode due to some intrinsic properties including excellent conductivity, low cost, and ease of modification [63]. In order to overcome several problems such as the fouling of electrodes and the high risk of interferences when using the naked graphite electrodes for the electrochemical detection of hazardous phenolic compounds, several studies have reported the modification of the graphite electrode with enzymes that also will be a benefit in improving the selectivity of the sensor [64].

Tyrosinase (Tyr), an enzyme that has a wide substrate specificity for phenolic compounds, has been widely fabricated in the graphite electrode-based electrochemical sensors for the detection of hazardous phenolic compounds [65,66]. A limit of detection (LOD) value of 0.4 μM for amperometric (AMP) detection of Ph was obtained using the Tyr-graphite electrode [67]. Tyr is able to catalyze the oxidation of Ph to quinones in the presence of oxygen. Subsequently, the generated quinones will be reduced to catechol that then will be measured as the electrochemical signal. Alongside Tyr, laccase (Lac) enzyme with the ability to oxidize many substrates by the reduction of oxygen to water also has been incorporated with graphite electrode. A wide linear range from 1000 to 10,000 μM has been exhibited by the Lac-modified graphite electrode for the AMP detection of Ph [68,69].

When a mediated Tyr-graphite electrode was used, the lower LOD of 0.006 μM was obtained [70]. As the graphite electrode was modified with tetracyanoquinodimethane first before Tyr was immobilized onto it, a linearity up to 25 μM and an LOD of 0.23 μM were obtained [71]. On the other hand, when 2-hexadecanol that worked as a solid binding matrix was included for the detection of Ph, a linear response up to 2.5 μM and an LOD of 0.2 μM were achieved [72]. In addition, a different approach of modifying the graphite electrode with carbodiimide first before Tyr is cross-linked onto it in the presence of glutaraldehyde (GA) has been used to improve the stability of the sensor [64].

In addition, some researchers have proposed the immobilization of the Tyr enzyme within a graphite–epoxy composite that offers high tolerance toward organic solvents, good mechanical stability, and fast response [73,74]. The graphite–epoxy composite also has been incorporated with horseradish peroxidase (HRP) enzyme for the square wave voltammetry (SWV) detection of Ph. When the SWV was coupled with the univariate

calibration method, weighted least squares, the obtained linear response, and LOD were 1.95–5.5 μM and 0.65 μM , respectively [75].

A comparison between three different glucose oxidase (GOD)–mutarotase reactor-graphite electrodes by immobilizing three different peroxidases, which are HRP, tobacco peroxidase, and peroxidase from peanut cell culture for AMP detection of Ph also has been done. The lowest LOD was exhibited by the HRP-modified graphite electrode with a value of $3.6 \pm 0.5 \mu\text{M}$ [76].

Several works have reported the incorporation between graphite and Teflon to serve as the immobilization matrix for enzymes including Tyr, HRP, and GOD as it offers several benefits such as high compatibility with organic solvents and remarkable long-term stability [77–79]. LOD values of 0.08 μM , 0.14 μM , and 7.6 μM were obtained using the developed graphite–Teflon–GOD–HRP–Tyr composite electrode for AMP detection of Ph, 2,4,6-TCP, and PCP, respectively [80].

Then, a new matrix for the immobilization of Tyr using graphite–ethylene/propylene/diene (EPD) was also introduced, and its performance was compared with the graphite–Teflon matrix for AMP sensing of Ph and 2,4-DMP. The graphite–EPD–Tyr composite electrode gave a better sensing performance toward both Ph and 2,4-DMP with LOD values of 26.3 nM and 0.67 μM , respectively. This might be due to the excellent signal-to-background ratios for analytes exhibited by the graphite–EPD–Tyr electrode [81].

As the presence of colloidal gold (Au) nanoparticles was able to enhance the kinetics of the reactions in electrochemical transduction, the nanoparticles were included in the fabrication of a Tyr–graphite–Teflon electrode for AMP sensing of Ph. This work resulted in an LOD value of 0.02 μM [82].

Some researchers have proposed an idea of immobilizing the enzymes onto the surface of a graphite-coated screen-printed four-channel Au electrode array and a screen-printed graphite electrode as the electrochemical sensors for hazardous phenolic compounds [83,84]. Researchers also have utilized the advantage of graphite pencil electrode of being unexpensive in the fabrication of electrochemical sensors. As the graphite pencil electrode has poor electrocatalytic properties toward 4-NP, it has been modified with copper. As a result, the AMP detection of 4-NP using the copper-modified electrode gave a lower LOD value of 1.9 μM compared to the bare electrode with a value of 1 mM [85].

Then, a new strategy for the detection of Ph was introduced by simply dipping a pre-charged graphite pencil electrode in the Ph solution to facilitate the electropolymerization of Ph without the need of any potential. The SVW response was increasing linearly to the Ph concentration over 0.05–1 μM [86]. As Au nanoparticles were employed into the pre-treated graphite pencil electrode, a broad linear response can be observed in the range of 0.5–100 μM for the detection of 4-NP [87].

A modifier also has been introduced in graphite paste electrode by synthesizing poly(dopamine-quinone chromium (III))-microspheres (PDQCM). A selective determination of Ph and 4-NP was achieved using the sensor, as the differential pulse voltammetry (DPV) of the simultaneous and individual determinations of the analytes showed no difference [88].

Graphite has been incorporated with dioctyl phthalate for the fabrication of a carbon paste electrode (CPE) that obtained an LOD of 2.5 μM for the voltammetric detection of Ph [89]. Furthermore, works based on the modification of glassy carbon electrode (GCE) also have been reported. GCE has been successfully modified with graphitized ordered mesoporous carbon that possesses several outstanding properties such as high specific surface area and pore volume [90]. A modification of GCE with graphite nanoflakes for the cyclic voltammetric (CV) detection of 4-NP gave an LOD of 0.18 μM [91].

On the other hand, an AMP sensor for Ph based on graphite-like carbon nitride (C_3N_4) has been successfully fabricated. However, as the graphite- C_3N_4 with low toxicity and excellent stability experienced poor conductivity, Au nanoparticles and cerium oxide have been used to overcome the drawback. An LOD of 2.33 μM and a linear response over 10–90 μM were obtained [92].

Table 1 summarizes the findings of graphite-based materials incorporated with electrochemical sensors for hazardous phenolic compounds detection.

Table 1. Graphite-based materials incorporated with electrochemical sensors for hazardous phenolic compounds detection.

Sensing Materials	Sensor	Hazardous Phenolic Compounds	Linear Range	LOD ¹	Ref.
Tyr-graphite electrode	Amperometry	Ph 2,4-DMP	0.02–0.14 mM 0.08–0.64 mM	6 µM 29 µM	[65]
Tyr-graphite electrode	Pulsed amperometry	Ph	Up to 2 mM	5.2 µM	[66]
Tyr-graphite electrode	Amperometry	Ph	Up to 600 µM	0.4 µM	[67]
<i>Trametes versicolor</i> laccase-graphite electrode	Amperometry	Ph	1000–10,000 µM	557 µM	[68]
<i>Cerrena unicolor</i> laccase-graphite electrode	Amperometry	Ph	1000–10,000 µM	296 ± 10 µM	[69]
Tyr-mediated graphite electrode	Amperometry	Ph	-	0.006 µM	[70]
Entrapped Tyr-tetracyanoquinodimethane-graphite electrode Immobilized Tyr-tetracyanoquinodimethane-graphite electrode	Amperometry	Ph	Up to 65 µM Up to 25 µM	- 0.23 µM	[71]
Tyr/graphite/2-hexadecanol	Chronoamperometry	Ph	Up to 2.5 µM	0.2 µM	[72]
Tyr-glutaraldehyde-carbodiimide-activated graphite electrode	Amperometry	Ph	0.01–5 µM	0.003 µM	[64]
Tyr-graphite-epoxy electrode	Amperometry	Ph	-	0.5 µM	[73]
Tyr-graphite-epoxy electrode	Amperometry	Ph	Up to 300 µM	1 µM	[74]
HRP-graphite-epoxy composite electrode	Square wave voltammetry/weighted least-squares Square wave voltammetry/partial least-squares 1	Ph	1.95–5.5 µM 1–62 µM	0.65 µM 1.1 µM	[75]
HRP-GOD-mutarotase reactor-graphite electrode Tobacco peroxidase-GOD-mutarotase reactor-graphite electrode Peroxidase from peanut cell culture-GOD-mutarotase reactor-graphite electrode	Amperometry	Ph	-	3.6 ± 0.5 µM 10.1 ± 0.8 µM 7 ± 0.6 µM	[76]
Graphite-Teflon-Tyr composite electrodes	Amperometry	Ph 2,4-DMP	4–80 µM 0.05–3 mM	1.1 µM 33.8 µM	[77]

Table 1. Cont.

Sensing Materials	Sensor	Hazardous Phenolic Compounds	Linear Range	LOD ¹	Ref.
Graphite–Teflon–HRP composite electrodes	Amperometry	2-CP	0.2–20 μM	0.16 μM	[78]
		2,4-DCP	0.4–20 μM	0.45 μM	
		2,4-DMP	4.5–10 μM	0.45 μM	
Graphite–Teflon–Tyr composite electrode	Flow injection with amperometry	Ph	0.01–40 μM	0.01 μM	[79]
	Flow injection with dual amperometry	2-CP	10–750 μM	7.3 μM	
Graphite–Teflon–GOD–HRP composite electrode	Flow injection with dual amperometry	Ph	0.25–50 μM	0.12 μM	
		Ph	1–100 μM	1.5 μM	
	Flow injection with amperometry	2-CP	1–50 μM	2.2 μM	
		2,4,6-TCP	1–50 μM	1.3 μM	
Flow injection with dual amperometry	Ph	1–100 μM	2.3 μM		
	2,4,6-TCP	5–60 μM	3 μM		
Sensing Materials	Sensor	Hazardous Phenolic Compounds	Linear Range	LOD ¹	Ref.
Graphite–Teflon–GOD–HRP–Tyr composite electrodes	Amperometry	Ph	0.1–20 μM	0.08 μM	[80]
		2,4,6-TCP	0.1–40 μM	0.14 μM	
		PCP	0.02–1000 μM	7.6 μM	
Graphite–Teflon–GOD–HRP composite electrodes	Amperometry	Ph	0.5–60 μM	0.43 μM	
		2,4,6-TCP	0.1–60 μM	0.11 μM	
Graphite–ethylene–propylene–diene–Tyr composite electrode	Amperometry	PCP	0.01–1500 μM	4.7 μM	
		Ph	0.05–6 μM	26.3 nM	
		2,4-DMP	1–50 μM	0.67 μM	
Graphite–Teflon–Tyr composite electrode	Amperometry	Ph	0.1–25 μM	99 nM	[81]
		2,4-DMP	0.7–100 μM	0.71 μM	
Tyr–colloidal gold nanoparticles–graphite–Teflon electrode	Amperometry	Ph	0.025–4 μM	0.02 μM	[82]
HRP–graphite-coated screen-printed four-channel gold-array	Amperometry	Ph	2–300 μM	-	[83]
Tyr–graphite-coated screen-printed four-channel gold-array			2–40 μM		
HRP–graphite-coated screen-printed four-channel gold-array			2–140 μM		

Table 1. Cont.

Sensing Materials	Sensor	Hazardous Phenolic Compounds	Linear Range	LOD ¹	Ref.
Tyr-screen-printed graphite electrode HRP/GOD-screen-printed graphite electrode	Amperometry	Ph	-	0.41 μ M 1.8 μ M	[84]
Copper-modified graphite pencil electrode Bare graphite pencil electrode	Amperometry	4-NP	50–850 μ M -	1.9 μ M 1 mM	[85]
Pre-charged disposable graphite pencil electrode	Square wave voltammetry	Ph	0.05–1 μ M	4.17 nM	[86]
Gold nanoparticles-pre-treated graphite pencil electrode Pre-treated graphite pencil electrode	Square wave voltammetry	4-NP	0.5–100 μ M 0.01–0.8 μ M	- 0.002 μ M	[87]
Poly(dopamine-quinone chromium (III))-microspheres/graphite paste electrode	Differential pulse voltammetry	Ph 4-NP	2.5–107.5 μ M 2.5–130 μ M	0.6 μ M 0.8 μ M	[88]
Graphite-dioctyl phthalate-CPE	Voltammetry	Ph	2.5 μ M–60 mM	2.5 μ M	[89]
Graphitized-ordered mesoporous carbon-Tyr-cobaltosic oxide nanorod-chitosan-GCE	Amperometry	Ph	0.05–11 μ M	0.025 μ M	[90]
Graphite nanoflakes-GCE	Cyclic voltammetry at peak c1 Cyclic voltammetry at peak a2	4-NP	0.5–6000 μ M 1–6000 μ M	0.18 μ M 0.7 μ M	[91]
Gold-cerium oxide-graphite-carbon nitride modified carbon paper	Amperometry	Ph	10–90 μ M	2.33 μ M	[92]

¹ where LOD is limit of detection. 2-CP: 2-chlorophenol, 2,4-DCP: 2,4-dichlorophenol, 2,4-DMP: 2,4-dimethylphenol, 2,4,6-TCP: 2,4,6-trichlorophenol, 4-NP: 4-nitrophenol, CPE: carbon paste electrode, GCE: glassy carbon electrode, GOD: glucose oxidase, HRP: horseradish peroxidase, PCP: pentachlorophenol, Ph: phenol, Tyr: tyrosinase.

2.1.2. Graphene

Graphene (Gr) has attracted a lot of attention due to its unique properties such as high charge transport mobility, excellent electrocatalytic activities, and good mechanical strength. A lot of researchers also have integrated Gr in the fabrication of electrochemical sensors due to these properties.

When Gr was incorporated with Nafion polymer in the development of a DPV sensor for 4-NP, an LOD of 0.6 μM was obtained [93]. A broad linearity from 4 to 800 μM with an LOD of 1.5 μM was achieved when palladium and ion liquid were included in the fabrication of a DPV sensor for 2-CP. The palladium was believed to be able to enhance the electrocatalytic activity for the oxidation of phenolic compound; meanwhile, the ion liquid acted as the linker [94].

Next, Gr nanosheets that possess remarkable electronic and mechanical properties were successfully exfoliated from graphite in the presence of *N*-methyl-2-pyrrolidone. When it was used to modify GCE as the DPV sensor for 4-NP, an LOD value of 0.04 μM was obtained [95]. Gr nanosheets that have been coupled with sodium dodecyl sulfate, a surfactant, have showed a great selectivity toward Ph in the presence of aminophenol and nitrophenol [96]. Surfactants are amphiphilic molecules that can be adsorbed on the interfaces of two phases with different polarities that thus will help to form a stable film [97].

On the other hand, Gr nanosheets that were incorporated with another surfactant, cetyltrimethylammonium bromide (CTAB), for DPV detection of 4-NP have achieved an LOD of 3 μM [98]. A broad linear range over 0.53–1063 μM was obtained for Ph when pure Gr was incorporated with CTAB [99]. In order to prevent the restacking of Gr, a modification of Gr with poly(sodium 4-styrenesulfonate) has been done. When the composite was incorporated with CTAB and Nafion on the surface of GCE, a low LOD value of 2 nM was obtained for the detection of 2,4-DCP [100].

Next, Gr nanosheets also have been modified with iron phthalocyanine, which is an electrocatalyst with a great electrocatalytic ability. As the iron phthalocyanine has a poor conductivity, pairing it with the Gr nanosheets will be a help to deliver its electrochemical properties. As a result, an LOD of 10 μM was exhibited using a CV sensor for the detection of 4-NP [101].

Some works have reported the modification of Gr with Au nanoparticles in order to combat the aggregation of Gr sheets that leads to the decrement of its surface area [102]. As a result, a low LOD value of 0.01 μM for the detection of 4-NP using the linear sweep voltammetry (LSV) method was achieved [103].

With the aim of improving the dispersion of Gr in an aqueous solution, chitosan (Chit), a natural and non-toxic biopolymer has been used [104]. When the Gr-Chit suspension was dropped on top of GCE, LOD values of 0.1 μM and 0.09 μM were obtained for the simultaneous LSV detection of 2-NP and 4-NP, respectively [105].

As Gr has a high surface area that is very beneficial for the immobilization of enzymes, some related works for the detection of hazardous phenolic compounds have been reported [106]. An excellent LOD value of 5 nM was achieved for the AMP detection of 2,4-DCP that was based on Gr, HRP enzyme, and Chit [107]. In addition, an incorporation between Gr, Tyr, Chit, and Au nanoparticles on a screen-printed carbon electrode was able to give an excellent selectivity toward Ph [108]. The work on silk peptide that works as a modifier to functionalize Gr also has been suggested. In the presence of Tyr, the AMP detection of Ph revealed that the current response was linearly dependent to its concentration over 0.0015–21.12 μM [109].

β -cyclodextrin (β -CD) is an oligosaccharide that is toroidal in shape with a hydrophobic inner cavity and a hydrophilic exterior. It has the ability to allow small guest molecules inside its hydrophobic cavity. Hence, β -CD has been widely used to improve the solubility and stability of Gr in the development of electrochemical sensors for hazardous phenolic compounds [110,111]. As the β -CD functionalized Gr was immobilized onto the surface of

CPE, an LOD of 0.2 μM for DPV detection of 2-CP was obtained. The schematic preparation of the pure β -CD functionalized Gr is as shown in Figure 2 [112].

However, the presence of β -CD has caused a decrease in the accessible active sites for the binding of target molecules. Carboxyl-multiwalled carbon nanotubes (MWCNTs) were proposed as the solution for this problem, as they have the ability to increase the electron transfer rate and contact area between the targets and the working electrode [113]. Furthermore, the adding of metal nanoparticles in the fabrication of electrochemical sensors for 4-NP based on the β -CD functionalized Gr-modified GCE has resulted in an excellent LOD value in the nanomolar range [114,115].

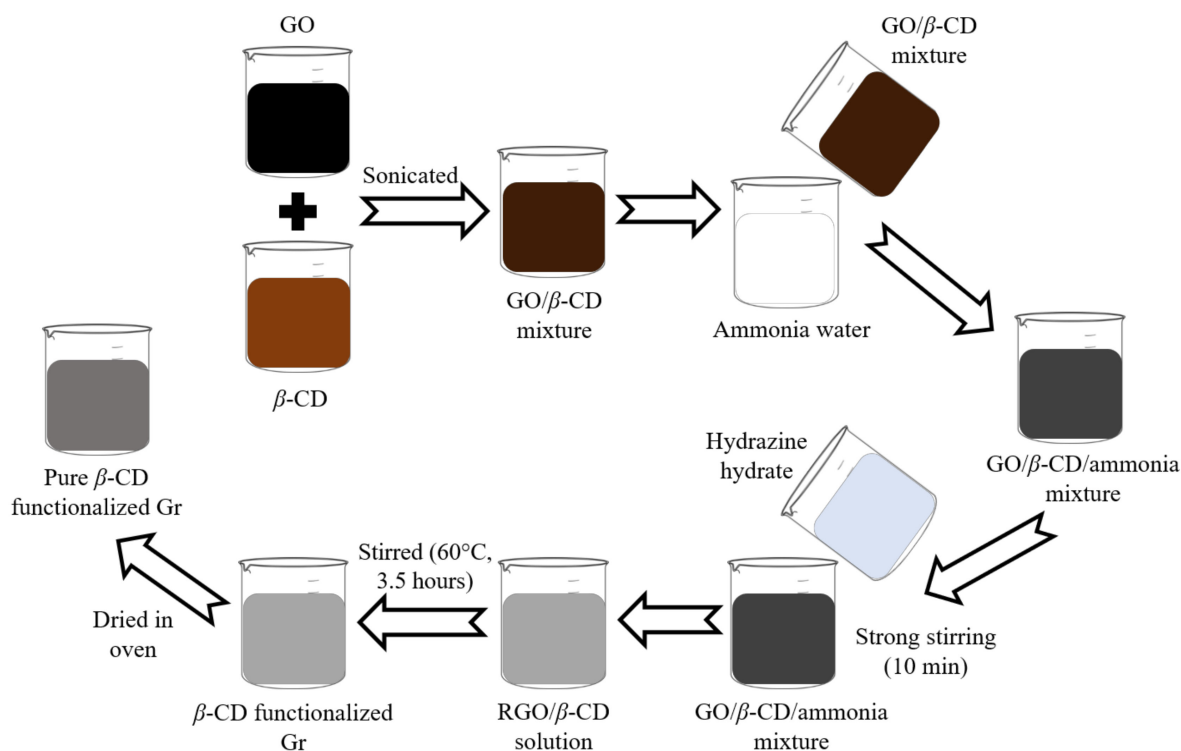


Figure 2. Schematic preparation of the pure β -CD functionalized Gr [112].

A low LOD of 0.008 μM has been achieved when Gr was incorporated with an acetylene black paste hybridized electrode for the LSV detection of 4-NP. This might be due to the high specific surface area and strong adsorption capacity of the acetylene black [116]. Next, hydroxyapatite with good adsorption capability has been integrated with Gr for 4-NP sensing that managed to give an LOD of 0.27 μM [117].

On the other side, two different regions of linear response in the range of 0.45–56 μM and 156–556 μM of Ph concentration were observed when incorporating Gr with Fe_3O_4 , which is a low toxic nanomaterial [118]. An LOD of 36.6 μM was obtained when Gr was immobilized onto the TiO_2 anatase-modified electrode for CV detection of Ph [119]. As nickel slag waste was included in the preparation of Gr- TiO_2 electrode, a lower LOD of 0.39 μM was achieved. This might be due to the great electrical conductivity and mechanical resistance of the nickel slag waste [120].

Gr-like carbon nitride that possesses a unique electronic structure and peculiar thermal stability has been successfully prepared through condensation reaction. Next, Na^+ was doped into the Gr-like carbon nitride to overcome the low conductivity experienced by the Gr-like carbon nitride. A linear AMP response for Ph over 10–110 μM with an LOD of 0.23 μM was achieved [121].

The summaries of Gr-based materials used for sensing hazardous phenolic compounds using electrochemical sensors are shown in Table 2.

Table 2. Gr-based materials incorporated with electrochemical sensors for hazardous phenolic compounds detection.

Sensing Materials	Sensor	Hazardous Phenolic Compounds	Linear Range	LOD ¹	Ref.
Gr-Nafion-screen-printed electrode	Differential pulse voltammetry	4-NP	10 μ M–0.62 mM	0.6 μ M	[93]
Ion liquid-palladium-Gr-Nafion-GCE	Differential pulse voltammetry	2-CP	4–800 μ M	1.5 μ M	[94]
<i>N</i> -methyl-2-pyrrolidone exfoliated Gr nanosheets-GCE	Differential pulse voltammetry	4-NP	-	0.04 μ M	[95]
Gr nanosheet paste electrode	Differential pulse voltammetry	Ph	0.08–80 μ M	0.05 μ M	[96]
Gr nanosheets-CTAB	Differential pulse voltammetry	4-NP	7.2–107.8 μ M	3 μ M	[98]
Gr-CTAB-GCE	Differential pulse voltammetry	Ph	0.53–1063 μ M	0.21 μ M	[99]
Nafion-poly(sodium 4-styrenesulfonate)-Gr-CTAB-GCE	Linear sweep voltammetry	2,4-DCP	0.01–2 μ M	2 nM	[100]
Gr nanosheets-iron phthalocyanine-GCE	Cyclic voltammetry	4-NP	0.1–0.7 mM	10 μ M	[101]
Gr-gold nanoparticles-GCE	Amperometry	4-NP	0.47–10,750 μ M	0.47 μ M	[102]
Gr-gold nanoparticles-GCE	Linear sweep voltammetry	4-NP	0.036–90 μ M	0.01 μ M	[103]
Gr-chitosan-acetylene black paste electrode	Linear sweep voltammetry	2-NP	0.4–80 μ M	0.2 μ M	[104]
		4-NP	0.1–20 μ M 20–80 μ M	0.08 μ M	
Gr-chitosan-GCE	Linear sweep voltammetry	2-NP	1–240 μ M	0.1 μ M	[105]
		4-NP	0.1–140 μ M	0.09 μ M	
Three-dimensional Gr-tyrosinase	Amperometry	Ph	0.05–2 μ M	0.05 μ M	[106]
Horseradish peroxidase-Gr-chitosan-GCE	Amperometry	2,4-DCP	0.01–13 μ M	5 nM	[107]
Gr-gold nanoparticles-chitosan-tyrosinase-screen-printed carbon electrode	Differential pulse voltammetry	Ph	0.05–15 μ M	0.016 μ M	[108]
		2,4-DCP	0.05–15 μ M	0.041 μ M	
		4-NP	0.05–19 μ M	0.031 μ M	
Tyrosinase-Gr-silk peptide-GCE	Amperometry	Ph	0.0015–21.12 μ M	0.35 nM	[109]
β -cyclodextrin-functionalized Gr nanosheets-GCE	Differential pulse voltammetry	2-NP	5–400 μ M	0.3 μ M	[110]
2-hydroxypropyl- β -cyclodextrin-Gr nanoribbon-GCE	Differential pulse voltammetry	2-CP	0.01–16 μ M	0.004 μ M	[111]
β -cyclodextrin-Gr-carbon paste electrode	Differential pulse voltammetry	2-CP	0.5–40 μ M	0.2 μ M	[112]
Carboxyl-multiwalled carbon nanotubes- β -cyclodextrin edge-functionalized Gr-GCE	Differential pulse voltammetry	4-NP	0.3–10 μ M 10–50 μ M	0.027 μ M	[113]

Table 2. Cont.

Sensing Materials	Sensor	Hazardous Phenolic Compounds	Linear Range	LOD ¹	Ref.
β -cyclodextrin functionalized Gr–silver–GCE	Amperometry	4-NP	0.01–0.1 μ M 0.1–1500 μ M	0.89 nM	[114]
β -cyclodextrin–gold@carboxylic Gr nanosheets–GCE	Differential pulse voltammetry	4-NP	0.01–5 μ M 5–200 μ M	3.8 nM	[115]
Gr–acetylene black paste hybridized electrode	Linear sweep voltammetry	4-NP	0.02–8 μ M 8–100 μ M	0.008 μ M	[116]
Magnetite–hydroxyapatite dispersed edge–carboxylated Gr–GCE	Cyclic voltammetry Differential pulse voltammetry	4-NP	30–1455 μ M 0.2–994 μ M	- 0.27 μ M	[117]
Fe ₃ O ₄ –amino functionalized Gr–GCE	Linear sweep voltammetry	Ph	0.45–56 μ M 156–456 μ M	0.4 μ M	[118]
Gr–TiO ₂ anatase–carbon paste electrode	Cyclic voltammetry	Ph	0.01–1 nM 1–1000 nM	36.6 μ M	[119]
Gr–nickel slag waste–TiO ₂ electrode	Voltammetry	Ph	1.06–10.63 μ M	0.39 μ M	[120]
Na ⁺ -doped Gr-like carbon nitride electrode	Amperometry	Ph	10–110 μ M	0.23 μ M	[121]

¹ where LOD is limit of detection. 2-CP: 2-chlorophenol, 2-NP: 2-nitrophenol, 2,4-DCP: 2,4-dichlorophenol, 4-NP: 4-nitrophenol, CTAB: cetyltrimethylammonium bromide, GCE: glassy carbon electrode, Gr: graphene, Ph: phenol.

2.1.3. Graphene Oxide

Graphene oxide (GO) is an insulating material with excellent optical and electrical properties that is soluble in water. Several groups that are present in GO including epoxy, hydroxyl, and carboxyl help provide GO with several characteristics such as hydrophilicity, high surface activity, and antifouling properties [122].

A simple work for the LSV detection of 4-NP based on GO-modified GCE was successfully developed. The estimated LOD was 0.02 μM , and a linear response in the range of 0.1–120 μM was observed [123]. A molecularly imprinted polymer (MIP) with high affinity toward the target analyte has been incorporated with the GO-modified GCE for the preparation of a DPV sensor for hazardous phenolic compounds. As a result, these sensors showed a great selectivity toward its target in the presence of several interferents [124,125].

Poly(ethyleneimine), a dendritic polymer, is an ideal material to be modified with GO as it consists of lots of amine groups that can interact with the epoxy groups of GO. The developed sensor is able to detect 2-NP down to 0.1 μM and has a good stability even after three months [126].

Nickel–curcumin that consists of phenolic active sites was chosen to be integrated with GO as it was believed to be able to enhance the electrocatalytic activity toward 4-NP. A linear increase in peak current with respect to an increase in the analyte concentration from 0.49 to 760 μM can be observed, and an LOD of 0.016 μM was estimated [127].

A great compatibility between GO and MWCNTs can be observed as the formed composite presents a larger surface area, faster electron transfer, and better stability. Then, GO and MWCNTs with negative charges have been paired up with poly(Rhodamine B) with positive charge and abundant active sites, which can be a help for the detection of hazardous phenolic compounds. The sensor gave LOD values of 0.8 nM and 0.5 nM for DPV detection of 2,4,6-TCP and PCP, respectively [128].

In order to enhance the electroanalytic properties of a DPV sensor for chlorophenols, a modification of GO with colloid carbon microspheres that are well-known for their excellent conductivity and monodispersity has been done. The presence of hydroxyl groups on colloid carbon microspheres makes them perfect activate sites for a noble metallic shell. LOD values in the nanomolar range were achieved [129].

Ionic liquid was used as a binder for a GO-Au nanoparticles hybrid to enhance the sensing performance of a DPV sensor toward 2,4-DCP. As a result, the modified sensor gave an LOD of 3 nM and exhibited good reproducibility, stability, and selectivity toward 2,4-DCP [130].

Some works have reported the incorporation of GO with several metal oxides such as zinc oxide (ZnO) and cuprous oxide (Cu_2O). The developed sensors presented high selectivity toward their target phenolic compounds [131,132].

Table 3 shows the findings of GO-based materials used for the detection of hazardous phenolic compounds using electrochemical sensors.

Table 3. GO-based materials incorporated with electrochemical sensors for hazardous phenolic compounds detection.

Sensing Materials	Sensor	Hazardous Phenolic Compounds	Linear Range	LOD ¹	Ref.
GO-GCE	Linear sweep voltammetry	4-NP	0.1–120 μM	0.02 μM	[123]
GO-molecularly imprinted polymer-GCE	Differential pulse voltammetry	2,4-DNP	1–150 μM	0.4 μM	[124]
Molecularly imprinted polymer-GO-GCE	Differential pulse voltammetry	2,4-DCP	0.004–10 μM	0.5 nM	[125]
GO-poly(ethyleneimine)-GCE	Square wave voltammetry	2-NP	5–155 μM	0.1 μM	[126]
GO/nickel-curcumin/GCE	Linear sweep voltammetry	4-NP	0.49–760 μM	0.016 μM	[127]
Poly(Rhodamine B)-GO-multiwalled carbon nanotubes-GCE	Differential pulse voltammetry	2,4,6-TCP	0.004–0.1 μM 0.1–100 μM	0.8 nM	[128]
		PCP	0.002–0.1 μM 0.1–90 μM	0.5 nM	
Core/shell structured carbon sphere-silver-GO-GCE	Differential pulse voltammetry	2-CP	0.05–25 μM	13.9 nM	[129]
		2,4-DCP	0.05–35 μM	7.52 nM	
		2,4,6-TCP	0.03–35 μM	9.71 nM	
Ionic liquid-GO-gold nanoparticles-GCE	Differential pulse voltammetry	2,4-DCP	0.01–5 μM	3 nM	[130]
GO-zinc oxide-GCE	Square wave voltammetry	Ph	5–155 μM	2.2 nM	[131]
Octahedral cuprous oxide-GO-GCE	Differential pulse voltammetry	4-NP	0.08–30 μM	8.5 nM	[132]

¹ where LOD is limit of detection. 2-CP: 2-chlorophenol, 2-NP: 2-nitrophenol, 2,4-DCP: 2,4-dichlorophenol, 2,4-DMP: 2,4-dimethylphenol, 2,4-DNP: 2,4-dinitrophenol, 2,4,6-TCP: 2,4,6-trichlorophenol, 4-NP: 4-nitrophenol, GCE: glassy carbon electrode, GO: graphene oxide, PCP: pentachlorophenol, Ph: phenol.

2.1.4. Reduced Graphene Oxide

Reduced graphene oxide (RGO) has received so much attention from researchers as it can be easily synthesized, is cost-effective, and has high conductivity. The availability of carboxyl and alcohol groups on its surface can work as binding sites for the sensing of hazardous phenolic compounds. Simple works by the reduction of GO to RGO directly on the surface of a working electrode for the development of electrochemical sensors for hazardous phenolic compounds have been reported [133,134]. When using GCE as the working electrode, an LOD of 0.55 μM for 4-NP using a DPV sensor was achieved [135].

In order to improve the electrochemical properties of RGO, a lot of works have reported the combination of RGO with β -CD in electrochemical sensors for the detection of nitrophenols [136]. As a result, low LOD values of 0.14 μM and 0.36 μM for DPV sensing of 2-NP and 4-NP were achieved, respectively [137]. As Chit was included in the fabrication of a DPV sensor for 2-NP and 4-NP, better sensing performance with lower LOD values of 0.018 μM and 0.016 μM were estimated for the analytes [138]. Furthermore, as the RGO/ β -CD/GCE was further modified with Prussian blue nanocubes, the LOD obtained for 4-NP can be lowered down to 2.34 nM. This might be owing to the ability of the Prussian blue to act as the electron-transfer mediator [139].

Due to the special characteristics of silver (Ag) nanoparticles such as excellent conductivity, low cost, and large surface area, they have been chosen to be incorporated with RGO on GCE for the detection of hazardous phenolic compounds [140,141]. Ag nanoparticles can help to improve the electrocatalytic activity of the hybrid material as it is able to facilitate more electron-transfer processes efficiently. A DPV sensor for the detection of PCP based on this combination of materials is able to obtain an LOD of 0.001 μM [142].

However, as Ag is well known for its chemical instability, some researchers have chosen to incorporate the RGO with Au nanoparticles. An LOD of 0.01 μM was obtained using a DPV sensor for the detection of 4-NP using the fabricated RGO-Au nanoparticles-modified GCE [143]. As Tyr was immobilized onto the RGO-Au nanoparticles-modified electrode for the AMP and chronoamperometric detection of Ph, a rather high LOD of 0.1 μM and 0.072 μM were exhibited, respectively [144,145].

The RGO-modified GCE has been used as the immobilization matrix for HRP and Lac enzymes for AMP detection of Ph. Three different linear slopes in the ranges of 0.05–0.1 mM, 0.2–1 mM, and 2–10 mM can be observed using the HRP-modified sensor [146]. Meanwhile, when RGO was mixed with Chit first before the immobilization of Lac, an LOD of 4.9 μM was determined [147].

As palladium nanoparticles possess superior catalytic activity toward the reduction of 4-NP, it has been incorporated with RGO that has resulted in a very low LOD of 9 fM [148]. In addition to metal nanoparticles, metal oxide nanoparticles also have been incorporated with RGO for the detection of 4-NP. When RGO was exploited with manganese oxide (MnO_2) nanoparticles, the sensor was highly selective toward 4-NP in the presence of several phenolic compounds with concentrations two times higher than 4-NP [149]. On the other hand, an LOD of 0.012 μM was obtained for 4-NP using a SWV sensor as RGO was incorporated with Fe_3O_4 nanoparticles. Fe_3O_4 nanoparticles played an important role in the prevention of Gr sheets from forming irreversible agglomerates [150].

Apart from that, ZnO metal oxide presents several unique properties such as low toxicity, a wide electrochemical potential window, and high chemical stability, and it also has been integrated with RGO for the modification of GCE [151,152]. As ZnO has a high band gap and RGO has a low band gap, nano-Schottky barriers will be formed at the RGO–ZnO interface. The sensitive detection of phenolic compounds can be achieved with the presence of the nano-Schottky barriers. By using the I–V method, an excellent LOD value of 0.27 nM was obtained for 2-NP sensing [153].

Next, a metal chalcogenide, copper sulfide djurleite, $\text{Cu}_{1.94}\text{S}$, was incorporated with RGO as a CV sensor for Ph that obtained a linear response in the range of 0.2–1.4 μM . The electronic mobility of the $\text{Cu}_{1.94}\text{S}$ was greatly enhanced when being modified with RGO [154].

An LSV sensor for 4-NP based on the doping of RGO with nitrogen gave an LOD of 0.007 μM [155]. A work based on the polymerization of 3,5-diamino-1,2,4-triazole on the surface of RGO-modified GCE exhibited broad linear responses at three different regions of 2–16 μM , 5–200 μM , and 300–1500 μM for the DPV sensing of 4-NP [156].

Next, polydopamine (PDA)–RGO-modified GCE has been successfully prepared considering the advantage of PDA that is rich in functional groups that can act as a platform for surface-mediated reactions. As MIP film was formed on the modified electrode surface, this sensor offered a high selectivity toward 2,4-DCP with an LOD of 0.8 nM [157].

In addition, a work has reported an LOD of 0.005 μM for the DPV detection of 2-NP. It was based on an urchin-like RGO-conjugated NiCo_2O_4 composite that was treated with 3-aminopropyltriethoxysilane that possesses superior electrochemical stability, good dispersibility, and a huge surface area [158].

The incorporations of RGO-based materials with electrochemical sensors for the detection of hazardous phenolic compounds is summarized in Table 4.

2.1.5. Graphene Quantum Dots

A DPV sensor for the detection of Ph based on a Au electrode was reported. As the Au electrode is easily disrupted by the surface-active compounds, it was then modified with graphene quantum dots (GQDs) and Au nanoparticles. A lower LOD value was exhibited by the GQDs–Au nanoparticles-modified Au electrode with a value of 0.44 μM compared to the bare electrode with 0.515 μM . This is attributed by the increase in electroactive surface area and charge transfer property. In addition, a broad linear response from 1 to 100 μM of Ph concentration was observed [159].

2.2. Extraction Methods with Chromatographic Analysis

2.2.1. Graphene

Gr has been applied as an adsorbent for sensing chlorophenols due to its benefit of having huge specific surface area that will be promising to increase the sorption capacity. The solid-phase extraction (SPE) technique with high recovery, high enrichment factor, and short extraction time has been used to extract the compounds first before it was detected using high-performance liquid chromatography (HPLC) and ultraviolet (UV) detection. The linear responses exhibited for 2-CP, 2,4-DCP, and 2,4,6-TCP were 7.78 nM to 1.56 μM , 6.13 nM to 1.23 μM , and 10.13 nM to 1.01 μM ; meanwhile, the LOD values were 1.56 nM, 1.23 nM, and 2.03 nM, respectively [160].

2.2.2. Graphene Oxide

Some works have reported the detection of chlorophenols based on GO as the adsorbent using magnetic solid-phase extraction (MSPE) as the extraction technique followed by HPLC-tandem mass spectrometry (MS). The first work has modified GO with a planar-structure amine-functional magnetic polymer to improve the low selectivity encountered by GO. The response was linear to the 2-CP, 2,4-DCP, 2,4,6-TCP, and PCP concentrations in the range of 0.08–3.89 nM, 0.03–1.23 nM, 0.01–1 nM, and 3.75–750.9 pM, respectively. The LOD values were evaluated to be 0.02 nM, 6.75 pM, 2.73 pM, and 0.6 pM for each of the analytes [161]. In order to overcome the difficulties of rapid separation of the samples, a planar GO-based magnetic ionic liquid nanomaterial was developed by modifying GO with $\text{Fe}_3\text{O}_4@\text{SiO}_2\text{-NH}_2$ microspheres. The obtained LOD for 2-CP, 2,4-DCP, 2,4,6-TCP, and PCP were 0.02 nM, 5.5 pM, 2 pM, and 0.5 pM, respectively. A linearity of 0.08–4 nM was observed for 2-CP, 0.03–3 nM for 2,4-DCP, 0.01–2.5 nM for 2,4,6-TCP, and 0.004–1.9 nM for PCP, respectively [162].

Table 4. RGO-based materials incorporated with electrochemical sensors for hazardous phenolic compounds detection.

Sensing Materials	Sensor	Hazardous Phenolic Compounds	Linear Range	LOD ¹	Ref.
RGO–screen-printed electrode	Electrochemical impedance spectroscopy	Ph	1–40 μM	0.2 μM	[133]
RGO–GCE	Differential pulse voltammetry	4-NP	50–800 μM	42 μM	[134]
RGO–GCE	Differential pulse voltammetry by oxidation reaction	4-NP	8.3–79.8 μM	2.13 μM	[135]
	Differential pulse voltammetry by reduction reaction		3.3–34.4 μM	0.55 μM	
Hydroxypropyl- β -cyclodextrin–RGO–GCE	Cyclic voltammetry	2-NP	0.05–100 μM	0.01 μM	[136]
β -cyclodextrin–RGO–GCE	Differential pulse voltammetry	2-NP	7.2–64.7 μM	0.14 μM	[137]
		4-NP	7.2–73 μM	0.36 μM	
RGO/ β -cyclodextrin/chitosan/GCE	Differential pulse voltammetry	2-NP	0.16–0.28 μM 5–40 μM	0.018 μM	[138]
		4-NP	0.06–0.16 μM 5–40 μM	0.016 μM	
β -cyclodextrin–Prussian blue nanocubes–RGO–GCE	Linear sweep voltammetry	4-NP	0.01–700 μM	2.34 nM	[139]
RGO–silver nanoparticles–GCE	Square wave voltammetry	4-NP	0.01–0.1 μM	1.2 nM	[140]
RGO–silver nanoparticles–GCE	Amperometry	4-NP	1–10 μM 10–110 μM 110–1110 μM	0.32 μM	[141]
Silver nanoparticles–RGO–GCE	Differential pulse voltammetry	PCP	0.008–10 μM	0.001 μM	[142]
Au nanoparticles–RGO–GCE	Differential pulse voltammetry	4-NP	0.05–2 μM 4–100 μM	0.01 μM	[143]
	Square wave voltammetry		0.05–2 μM	0.02 μM	
Tyrosinase–RGO–Au nanoparticles–Au/chromium electrode	Amperometry	Ph	-	0.1 μM	[144]
Au nanoparticles–RGO–tyrosinase–indium tin oxide electrode	Chronoamperometry	Ph	Up to 19.5 μM	0.072 μM	[145]
Horseradish peroxidase–partially RGO–GCE	Amperometry	Ph	0.05–0.1 mM 0.2–1 mM 2–10 mM	4.4 μM	[146]

Table 4. Cont.

Sensing Materials	Sensor	Hazardous Phenolic Compounds	Linear Range	LOD ¹	Ref.
RGO–chitosan–laccase–GCE	Amperometry	Ph	5–30 μ M	4.9 μ M	[147]
Palladium nanoparticles–RGO–gum arabic–GCE	Linear sweep voltammetry	4-NP	20–400 pM	-	[148]
	Electrochemical impedance spectroscopy		5–300 pM	2 pM	
	Square wave voltammetry		2–80 pM	9 fM	
Manganese dioxide nanoparticles–RGO–GCE	Linear sweep voltammetry	4-NP	0.02–0.5 μ M 2–180 μ M	0.01 μ M	[149]
RGO–Fe ₃ O ₄ nanoparticles–GCE	Differential pulse voltammetry	4-NP	0.2–10 μ M	0.26 μ M	[150]
	Square wave voltammetry		20–100 μ M 0.2–10 μ M	0.012 μ M	
RGO–zinc oxide–GCE	Differential pulse voltammetry	Ph	2–15 μ M 15–40 μ M	1.94 μ M	[151]
RGO–zinc oxide nanoflowers–GCE	Linear sweep voltammetry	4-NP 2,4-DNP	0.2–0.9 mM 0.1–0.9 mM	0.93 μ M 6.2 μ M	[152]
RGO–zinc oxide–GCE	I-V method	2-NP	0.01–10,000 μ M	0.27 nM	[153]
Copper sulfide djurleite–RGO–GCE	Cyclic voltammetry	Ph	0.2–1.4 μ M	-	[154]
Nitrogen-doped–RGO–GCE	Linear sweep voltammetry	4-NP	0.02–0.5 μ M	0.007 μ M	[155]
Polymerized 3,5-diamino-1,2,4-triazole/RGO/GCE	Differential pulse voltammetry	4-NP	2–16 μ M 5–200 μ M 300–1500 μ M	0.037 μ M	[156]
Molecularly imprinted polymer–polydopamine–RGO–GCE	Differential pulse voltammetry	2,4-DCP	2–10 nM 10–100 nM	0.8 nM	[157]
RGO/NiCo ₂ O ₄ /3- aminopropyltriethoxysilane/GCE	Differential pulse voltammetry	2-NP	0.005–0.5 μ M 1–25 μ M	5 nM	[158]

¹ where LOD is limit of detection. 2-NP: 2-nitrophenol, 2,4-DCP: 2,4-dichlorophenol, 2,4-DNP: 2,4-dinitrophenol, 4-NP: 4-nitrophenol, Au: gold, GCE: glassy carbon electrode, PCP: pentachlorophenol, Ph: phenol, RGO: reduced graphene oxide.

On the other hand, Chen et al. encountered the same problem and incorporated GO with triethylenetetramine-functionalized magnetic particles as an adsorbent for the MSPE of PCP and 4-NP that was then detected using liquid chromatography and tandem MS. The linear response obtained for both analytes was 0.02–7.2 nM, and the LOD was in the range of 1–11 pM [163].

Furthermore, some researchers have introduced GO-based magnetic nanosorbents for the detection of hazardous phenolic compounds. In a work, GO has been modified with Fe₃O₄-SiO₂ magnetic nanoparticles to encourage a uniform energy transfer and accelerate the reaction with Ph and 4-NP as the target analytes. The targets were firstly extracted using dispersive SPE and detected using HPLC-UV detection. A linear response was exhibited by Ph in the range of 0.01–1 µM; meanwhile, 4-NP showed a wider linearity from 7.16 to 716 nM. A slightly lower LOD was estimated for Ph with a value of 5.3 nM compared to 4-NP with 5.75 nM [164]. Another work reported the preparation of GO/Fe₃O₄/di-(2-ethylhexyl) phosphoric acid composite as the MSPE adsorbent for Ph. Then, the Ph was detected using HPLC-UV detection where an LOD value of 5.3 nM and a dynamic linear response from 0.5 to 53 nM were achieved [165].

Another magnetic nanosorbent was developed by modifying GO with Fe-Fe₂O₃ nanowires to increase the hydrophilicity and dispersibility of GO in aqueous solution. The composite was used for the MSPE of 2,4-DCP coupled with HPLC-UV detection. This developed sensor gave a good linearity over the 2,4-DCP concentration range between 3.07 and 613.5 nM with an LOD of 0.61 nM [166].

The solid-phase microextraction (SPME) method also has been introduced for the extraction of the hazardous phenolic compounds. SPME is a simple, fast, and solvent-free technique that combines sampling, isolation, and enrichment into a single step. A modification of GO with polyethylene glycol to be used as the fiber coating of the SPME process of 2,4-DMP has been reported. Using flame ionization detection (FID), a low LOD of 0.08 nM with a linear response from 0.4 to 1640 nM were observed [167].

As GO experienced a drawback of low thermal stability, it has been modified with polyoxyethylene, which is a highly cross-linked substrate for the preparation of another fiber coating for headspace (HS)-SPME coupled with the GC-MS detection of chlorophenols. The linearity obtained for 2-CP, 2,4-DCP, and 2,4,6-TCP were 0.03–7.8 nM, 0.03–6 nM, and 0.05–5 nM, respectively. LOD values of 1 pM, 1.9 pM, and 6.9 pM were estimated for each of the analytes, respectively [168].

A GO-reinforced polymeric ionic liquids monolith also has been developed for the SPME of 2,4,6-TCP and 2-NP followed by HPLC. It was prepared by the polymerization of GO-doped amino- and benzyl-functionalized 1-(3-aminopropyl)-3-(4-vinylbenzyl)imidazolium 4-styrenesulfonate monomer with the help of a cross-linking agent, 1,6-di-(3-vinylimidazolium) hexane bihexafluorophosphate. The linear response and LOD obtained for 2,4,6-TCP were 5–2030 nM and 1 nM; meanwhile, the values were 0.04–3 µM and 4 nM for 2-NP, respectively [169].

2.2.3. Reduced Graphene Oxide

Over the years, only one work has been reported for the SPE of hazardous phenolic compounds using RGO. The extraction of the targets was followed by HPLC-UV detection. To overcome several challenges such as the low sorption capacity and extraction efficiency when directly using RGO as the sorbent, the RGO has been immobilized onto an encapsulated silica, SiO₂. The linear responses observed were in the range of 0.08–4 µM for 2-CP, 0.03–3 µM for 2,4-DCP, 0.03–2.5 µM for 2,4,6-TCP, and 0.02–2 µM for PCP, respectively. LOD values of 0.03 µM, 0.009 µM, 0.006 µM, and 0.005 µM were estimated for 2,CP, 2,4-DCP, 2,4,6-TCP, and PCP, respectively [170].

2.3. Optical Sensors

2.3.1. Graphene

A series of works for the detection of PCP using a Gr-based electrochemiluminescence (ECL) sensor were reported by the researchers. The first one was based on the incorporation of Gr with carbon quantum dots (CQDs). Owing to the superior electrical conductivity and electrocatalytic activity of Gr, the low ECL intensity of CQDs was greatly improved, and the PCP was detected as low as 1 pM with a broad linear response over the range of 1–10,000 pM [171]. Gr has played an important role in combating the problem of non-recyclable Au nanoclusters by acting as the signal amplifier. As the PCP concentration increased from 0.01 to 100 pM, the ECL intensity also increased. A low LOD of 0.01 pM was achieved [172]. Another work has reported the incorporation of ZnO nanocrystals on nitrogen-doped Gr nanocomposites-modified GCE. The nitrogen-doped Gr played an important role in enhancing the ECL intensity by 4.3-fold and moving the onset ECL potential more positively. This has resulted in a low LOD value of 0.16 pM for PCP with a broad linear response from 0.5 pM to 61.1 nM [173].

On the other hand, a colorimetric sensor for the detection of 4-NP based on a three-dimensional Gr foam/mesoporous-Fe₃O₄ nanohybrid was successfully prepared via the solvothermal method. The adding of Gr in the development of this sensor was to tackle the drawback of Fe₃O₄ nanozymes that are easy to aggregate, leading to the losses of their catalytic activity. Then, the sensor exhibited linear responses between 0.1–10 μM and 10–1000 μM and gave an LOD of 0.045 μM [174].

2.3.2. Graphene Oxide

The only reported work incorporating GO with an optical sensor was for the detection of Ph using a surface plasmon resonance (SPR) sensor. A layer of GO modified Tyr enzyme was coated on the top of the Au thin film to improve the sensitivity of the SPR sensor to the low concentration of phenol. As the incident light from the He-Ne laser beam hits the GO–Tyr–Au thin film, the free electrons at the interface will absorb the light, causing them to resonate. The resonating electrons will form electromagnetic waves that are known as surface plasmons, which propagate parallel to the metal surface. Hence, at a specific incident angle, resonance will occur as the momentum of the surface plasmon is equivalent to the momentum of incident photon [175,176]. Consequently, a sharp shadow called SPR can be observed [177]. This fabricated sensor was able to detect Ph down to 1 μM, and a linear response can be observed from 0 to 100 μM [178].

2.3.3. Reduced Graphene Oxide

An ECL sensor for the detection of PCP was fabricated by using RGO as the immobilization substrate for cadmium sulfide nanowires to improve the stability and recyclability of the luminophore. The ECL intensity was linearly dependent on the PCP concentration in a wide range of 0.01–10,000 pM, and the LOD obtained was as low as 2 fM [179].

Next, a “turn-on” fluorescence sensor for Ph based on RGO/polystyrenesulfonate/dextran–fluorescein was successfully developed. Due to the close proximity between the surface of the RGO and dextran–fluorescein (fluorophore probe) that causes rapid energy transfer from the fluorophore to RGO, a completely quenched fluorescence was achieved. The sensor gave a linearity over a broad concentration of Ph from 0.01 to 1000 nM, and the LOD value was 7.2 pM [180].

Au–nickel bimetallic nanoparticles loaded RGO has been developed as a design of a colorimetric sensor for Ph sensing. In the presence of hydrogen peroxide, the colorimetric assay based on the oxidative coupling of Ph and 4-aminoantipyrine turned from colorless to pink color quickly. The response of the sensor was linearly dependent on the Ph concentration over 0–300 μM and gave an LOD of 1.68 μM. This sensor was highly selective toward Ph in the presence of several interfering substances, which were 20 times higher in concentration [181]. Another colorimetric sensor for Ph was established by introducing a metal organic framework to the Fe₃O₄ nanoparticles–RGO composite. The absorbance

increased when the Ph concentration increased over 10–100 μM , and the LOD was calculated to be 3.33 μM . An excellent selectivity for Ph was exhibited by this sensor as it did not interfere with any tested control solutions [182].

2.3.4. Graphene Quantum Dots

GQDs have been widely fabricated in optical sensors due to their unique properties such as low toxicity, high fluorescent activity, excellent photoluminescence, and good biocompatibility [183]. A GQDs-based resonance light scattering sensor for the detection of Ph has been reported. In the presence of HRP and hydrogen peroxide, the developed sensor gave a low LOD of 22 nM, and the linear response can be observed in two parts, from 0.06 to 2.16 μM and between 2.4 and 28.8 μM . In addition, no noticeable interference effect can be observed when it was tested with some common anions and phenol homologues [184].

A colorimetric sensor for the detection of 4-NP has been prepared based on sulfur-doped GQDs-modified Au nanoparticles. When the detection of 4-NP was run in deionized water, the absorbance intensity was in a linear relationship to its concentration over 0.005–1 μM and 1–50 μM and gave an LOD of 3.5 nM. When the detection is examined in wastewater, a higher LOD of 8.4 nM was exhibited with linear responses in the range of 0.01–1.8 μM and 1.8–50 μM [185].

Some researchers have chosen to incorporate GQDs with a fluorescent sensor for the detection of 4-NP. In addition to having its own advantages of simple sample pre-treatment and low amount of solvent required, this fluorescent method is also able to overcome the problem encountered by the conventional fluorescent methods that require inducers or derivatizations. Zhou et al. have modified the GQDs with imprinted silica film to improve the selectivity of the sensor. As a result, this sensor was highly selective toward 4-NP even when tested with 2-NP that has similar properties as 4-NP. The fluorescence intensity was increasing linearly to the 4-NP concentration in the range of 0.14–21.57 μM and exhibited an LOD of 64.7 nM [186]. Meanwhile, Anh et al. have doped the GQDs with sulfur atoms to amplify the photoluminescence behavior of the GQDs that consequently will help improve the selectivity of the sensor. A lower LOD was obtained in deionized water with a value of 0.7 nM compared to wastewater with 3.5 nM. Both detections of 4-NP gave two different linear parts with values of 0.01–1 μM and 1–200 μM in deionized water, and 0.05–1 μM and 1–200 μM in wastewater, respectively. Even when tested with interferents with a concentration four times higher than the 4-NP, the F/F_0 ratio remains the same, proving the excellent selectivity of the sensor toward 4-NP [187].

3. Conducting Polymers-Based Materials Incorporated with Various Sensors for the Detection of Hazardous Phenolic Compounds

To date, most of the works on the detection of hazardous phenolic compounds that have been reported by the researchers were based on polypyrrole, polyaniline, and poly(3,4-ethylenedioxythiophene) (a 3,4-disubstituted polythiophene) among the conducting polymers. This is due to the high sensitivity offered by the conducting polymers in the field of sensors [188]. Although poly(diaminonaphthalene) and polyterthiophene have been widely used in the fabrication of sensors for the detection of glucose, dopamine, and more [189–195], interestingly, there is no work reported on the sensing of hazardous phenolic compounds. Hence, this section will be focusing on the incorporation of polypyrrole, polyaniline, and poly(3,4-ethylenedioxythiophene)-based materials with various sensors for hazardous phenolic compounds sensing.

3.1. Electrochemical Sensors

3.1.1. Polypyrrole

Polypyrrole (PPy) was widely used as the sensing layer in the development of sensors thanks to its environmental stability, high electron affinity, and remarkable electronic properties [196]. When PPy is used to modify the GCE for the HS-voltammetric detection of Ph, a low LOD of 0.07 μM was obtained [197].

The fabrication of biosensors has become a favorite thing among researchers around the world as biosensors offer high selectivity toward the target analytes and simple use for continuous on-site analysis. However, the direct use of the enzymes on working electrodes for electrochemical sensing application experienced several drawbacks of enzyme desorption and low stability. In order to overcome these problems, the enzymes must be immobilized on a suitable support matrix.

Hence, a lot of studies have reported PPy as the immobilization matrix for the enzymes in the development of electrochemical sensors for the detection of hazardous phenolic compounds [198–201]. The first work that has been proposed on the Tyr-immobilized PPy-modified GCE obtained a low LOD of 5 nM for the AMP detection of Ph [202]. On the other hand, when CPE was used as the working electrode, a linear response up to 7 μM of Ph concentration was observed [203]. A low LOD of 14.4 nM was obtained when polyphenol oxidase (PPO) was incorporated with PPy nanotubes derived from methyl orange [204].

A combination of PPy and *o*-amino-benzenesulfonic acid, a derivative of polyaniline, on the surface of a platinum (Pt) electrode also has been done. The response was increasing linearly to Ph concentration up to 100 μM for both AMP and pulsed AMP mode of detections [205].

Another AMP work for Ph sensing was conducted by comparing the performance of the PPy-Tyr-modified electrode with and without the cross-linking with GA. In the end, both of the electrodes that work in aqueous and chloroform showed a linearity up to 7 mM and 2.5 mM, respectively [206]. As polyglutaraldehyde (PGA) and HRP enzyme were used instead of GA and Tyr, a wider linear response over 16–112 μM was obtained [207].

Next, a series of works for the AMP sensing of Ph have been successfully reported. The immobilization of Tyr on *p*-toluene sulfonate ion-doped PPy gave an LOD of 0.8 μM [208]; meanwhile, the incorporation between Tyr and poly(*N*-3-aminopropyl pyrrole-co-pyrrole) on an indium tin oxide (ITO) electrode gave a lower LOD of 0.7 μM [209]. When *N*-amino substituted PPy film is being used as the support matrix for Tyr, an LOD of 0.9 μM was estimated [210]. As Tyr was entrapped on the $\text{Fe}(\text{CN})_6^{4-}$ -doped PPy-modified ITO electrode, a high LOD of 2.9 μM was achieved [211]. However, a lower LOD of 0.7 μM was obtained when the pyrrole was polymerized in the presence of both $\text{Fe}(\text{CN})_6^{4-}$ and Tyr on the ITO electrode [212].

Au nanoparticles that showed great compatibility with PPy also have been reported in the development of an AMP sensor for Ph. The electrochemical responses of the hybrid materials can be enhanced owing to the large specific surface area and high conductivity of Au nanoparticles. When the PPy–Au nanoparticles-modified GCE became an immobilization matrix for Tyr and HRP enzymes, a lower LOD was obtained by the Tyr enzyme with a value of 0.03 μM compared to the HRP with 15 μM [213,214]. This proved that the Tyr had better sensitivity toward Ph detection compared to HRP.

In order to further improve the stability of enzymes in the PPy-based AMP biosensors, researchers have included MWCNTs in the fabrication of the sensors as it is capable of facilitating direct electrochemical analysis of enzymes. A slightly lower LOD was obtained for Ph sensing when incorporating an Lac–PPy-modified electrode with MWCNTs compared to the one without MWCNTs with values of 0.03 μM and 0.04 μM , respectively. When a redox mediator was included, a broader linear response of 0.2–2.56 μM was observed [215].

On the other hand, as HRP was immobilized on the PPy–MWCNTs-modified Au electrode, LOD values of 3.52 μM , 0.26 μM , and 27.9 μM were obtained for Ph, 2-CP, and 2,4-DMP, respectively. As PPy encountered some instability at its cationic sites, sodium dodecyl sulfate has been used as the supporting electrolyte during the electropolymerization of pyrrole [216]. Lower LOD values of 0.732 μM , 0.249 μM , and 0.382 μM were obtained for each of the analytes, as a poly(glycidyl methacrylate-co-3-methylthienyl methacrylate) (poly(GMA-co-MTM)) copolymer was included in the fabrication of the AMP sensor. This might be due to the presence of epoxy groups in the poly(GMA-co-MTM) that are able to enhance the stability of the HRP enzyme on the working electrode. Figure 3 shows the schematic preparation of the sensor [217].

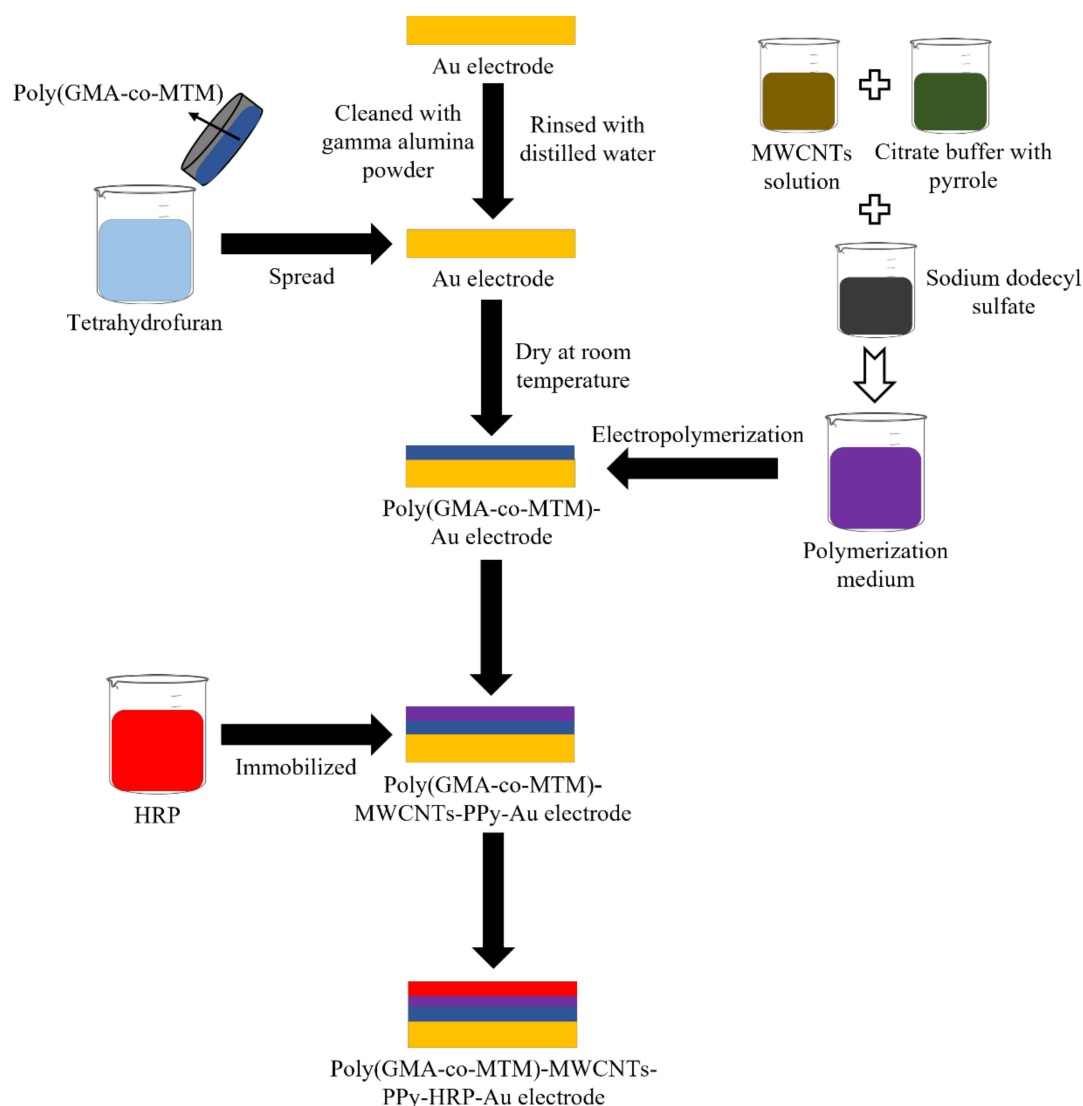


Figure 3. Schematic illustration of preparation of the poly(GMA-co-MTM)-MWCNTs-PPy-HRP-Au electrode [217].

A homopolymer, polyvinylferrocene, has been used to improve the electrical and thermal stability of PPy. The conductivity of PPy also can be greatly enhanced through this modification. Polyvinylferrocene also has high capability for minimizing the denaturation of enzymes. Using the HRP enzyme as the enzyme model, an LOD of 0.23 μM was obtained for AMP detection of Ph, and the developed sensor was able to retain 60% of its initial enzyme activity after two months stored at 4 $^{\circ}\text{C}$ [218]. Next, a redox polymer based on the copolymerization of vinylferrocene with glycidyl methacrylate has been successfully designed. Then, Tyr was immobilized on the surface of the copolymer-PPy-based GCE in the presence of PGA. An LOD of 0.781 μM was obtained [219].

An AMP sensor for Ph that was proposed based on the modification of PPy with polyvinylsulfonate for the immobilization of Tyr has obtained an LOD of 10 nM. A good stability was offered by the sensor after 45 days that might be owing to the presence of polyvinylsulfonate that acts as stabilizer [220].

An incorporation between nano PPy and sodium dodecyl sulfate film for the SWV detection of 4-NP also has been done. The film that possesses a hydrophobic nature has interacted with the 4-NP, which is hydrophobic in nature through hydrophobic force. As a result, a low LOD of 0.1 nM was achieved [221].

The findings of PPy-based materials used in the development of electrochemical sensors for the detection of hazardous phenolic compounds are shown in Table 5.

Table 5. PPy-based materials incorporated with electrochemical sensors for hazardous phenolic compounds detection.

Sensing Materials	Sensor	Hazardous Phenolic Compounds	Linear Range	LOD ¹	Ref.
PPy-GCE	Headspace-voltammetry	Ph	0.25–1.25 μM	0.07 μM	[197]
PPy-PPO-GCE	Amperometry	Ph 2-CP 2,4-DCP 2,4,6-TCP PCP	0.01–70 μM - -	0.1 μM 0.2 μM 0.4 μM 0.2 μM 0.2 μM	[198]
PPy-Tyr-GCE PPy-Tyr-HRP-GCE	Amperometry	Ph	0.06–125 μM 0.24–125 μM	-	[199]
PPy-Tyr-GCE	Amperometry	Ph	Up to 10 μM	10 nM	[200]
PPy-Tyr-GCE	Amperometry	Ph	-	5 nM	[202]
PPy-Tyr-CPE	Amperometry	Ph	Up to 7 μM	-	[203]
PPy nanotubes-PPO-GCE	Amperometry	Ph	0.5–40 μM	14.4 nM	[204]
PPy-o-amino-benzenesulfonic acid-Pt electrode	Amperometry Pulsed amperometry	Ph	Up to 100 μM	0.5 μM 0.1 μM	[205]
PPy-Tyr-Pt electrode in aqueous PPy-Tyr-GA-Pt electrode in aqueous PPy-Tyr-Pt electrode in chloroform PPy-Tyr-GA-Pt electrode in chloroform	Amperometry	Ph	Up to 7 mM Up to 2.5 mM	0.8 nM - 50 nM -	[206]
Polyglutaraldehyde-PPy-HRP-gold electrode	Amperometry	Ph 2-CP	16–112 μM 4–128 μM	0.087 μM 0.114 μM	[207]
Tyr/p-toluene sulfonate ion-PPy/GCE	Amperometry	Ph	3.3–220.3 μM	0.8 μM	[208]
Tyr-poly(N-3-aminopropyl pyrrole-co-pyrrole)-ITO electrode	Amperometry	Ph	1.35–222.3 μM	0.7 μM	[209]
Tyr-N-amino substituted PPy electrode	Amperometry	Ph	1.8–170.2 μM	0.9 μM	[210]
Tyr/Fe(CN) ₆ ⁴⁻ -PPy/ITO electrode	Amperometry	Ph	9.9–84.7 μM	2.9 μM	[211]
Tyr/Fe(CN) ₆ ⁴⁻ -PPy/ITO electrode	Amperometry	Ph	4.5–107.4 μM	0.7 μM	[212]
PPy-Tyr-gold nanoparticles-GCE	Amperometry	Ph	0.25–70 μM	0.03 μM	[213]
PPy-HRP-gold nanoparticles-GCE	Amperometry	Ph	0.01–0.2 mM	15 μM	[214]

Table 5. Cont.

Sensing Materials	Sensor	Hazardous Phenolic Compounds	Linear Range	LOD ¹	Ref.
Lac-PPy-GCE	Amperometry	Ph	0.2–1.4 μM	0.04 μM	[215]
Lac-PPy-MWCNTs-GCE			0.39–1.4 μM	0.03 μM	
Lac-PPy-MWCNTs-Prussian blue-GCE			0.2–2.56 μM	0.03 μM	
MWCNTs-PPy-HRP-gold electrode	Amperometry	Ph	16–44 μM	3.52 μM	[216]
		2-CP	1.6–8 μM	0.26 μM	
		2,4-DMP	64–240 μM	27.9 μM	
Poly(glycidyl methacrylate-co-3-methylthienyl methacrylate)-MWCNTs-PPy-HRP-gold electrode	Amperometry	Ph	1.6–72 μM	0.732 μM	[217]
		2-CP	1.6–68.8 μM	0.249 μM	
		2,4-DMP	1.6–40 μM	0.382 μM	
HRP-PPy-polyvinylferrocene-GCE	Amperometry	Ph	0.5–10 μM	0.23 μM	[218]
Tyr-poly(glycidyl methacrylate ₈₅ -co-vinylferrocene ₁₅)-polyglutaraldehyde-PPy-GCE	Amperometry	Ph	20–70 μM	0.781 μM	[219]
PPy-polyvinylsulfonate-Tyr-Pt electrode	Amperometry	Ph	0.1–5 μM	10 nM	[220]
Nano PPy-sodium dodecyl sulfate film modified GCE	Square wave voltammetry	4-NP	0.1 nM–100 μM	0.1 nM	[221]

¹ where LOD is limit of detection. 2-CP: 2-chlorophenol, 2,4-DCP: 2,4-dichlorophenol, 2,4-DMP: 2,4-dimethylphenol, 2,4,6-TCP: 2,4,6-trichlorophenol, 4-NP: 4-nitrophenol, GA: glutaraldehyde, GCE: glassy carbon electrode, HRP: horseradish peroxidase, ITO: indium tin oxide, Lac: laccase, MWCNTs: multiwalled carbon nanotubes, PCP: pentachlorophenol, Ph: phenol, PPO: polyphenol oxidase, PPy: polypyrrole, Pt: platinum, Tyr: tyrosinase.

3.1.2. Polyaniline and Its Derivative

Polyaniline (PANI) has high conductivity, good environmental stability, and also has been actively fabricated in electrochemical sensors for hazardous phenolic compounds. As PANI might be inactive or experiencing the decline of its activity at high pH value, some researchers have chosen to do an optimization study for the effect of pH on the sensing performance of the fabricated PANI-based sensors. The optimum pH might differ according to the combination of materials that they used. All of the related works found out that the optimum pH for the PANI-based sensors was below the neutral pH.

PANI nanosheets that received a lot of attention in the field of sensors have been utilized in a cyclic voltammetric sensor for Ph sensing. The sensor gave an LOD of 4.43 μM , and a considerable stability was exhibited, as it did not show any noticeable decrease in the sensing properties when tested for three consecutive weeks [222].

Several studies have reported the use of PANI as the solid support for the immobilization of enzymes mainly for the detection of Ph using an AMP sensor in order to improve the selectivity of the sensors [223,224]. A good selectivity toward Ph was observed when Tyr was immobilized onto a PANI-modified Pt electrode. The sensor also showed a great sensitivity as a low LOD of 10 nM was obtained [225].

However, these AMP biosensors that incorporated PANI experienced a huge reduction of background current that limits its sensing application. Hence, an initiative has been taken by modifying the PANI with polyacrylonitrile to overcome the drawback that consequently will lead to a more stable sensor. A sensitivity of 0.96 $\text{A M}^{-1} \text{cm}^{-2}$ was obtained for Ph sensing [226].

With the aim of enhancing the conductivity of the PANI-based AMP biosensor, PANI has been integrated with ionic liquid and carbon nanofibers. As a result, an LOD of 0.1 nM was achieved as the composite showed a fibrillar morphology, which is the main key to improve the capacity of Tyr enzyme loading [227].

An AMP sensing of Ph by the modification of CPE using PANI and activated carbon also has been reported. Using Tyr as the enzyme model, the sensor was highly selective toward Ph in the presence of several cations such as Pb^{2+} , Cr^{5+} , and Ni^{2+} [228].

Next, an electrochemical–chemical–chemical redox cycling work with a sulfonated PANI–Chit composite as the redox capacitor to transfer electron has been developed. A low LOD of 0.8 nM was achieved using Tyr as the immobilized enzyme [229].

Some researchers have reported enzymeless PANI-based electrochemical sensors, as enzymes have some disadvantages such as being expensive and difficulty storing. A CV sensor for 4-NP was developed by doping PANI with polyvinyl sulfonic acid to improve the stability of the sensor. MIP is also included to improve its selectivity through the overoxidation process to remove the embedded 4-NP molecules from the composite. As a result, the sensor had a shelf-life of 45 days and did not give any noticeable changes in the presence of interferents [230].

Another CV sensor for 4-NP was fabricated by preparing nanostructured carbonized PANI, which is an excellent catalyst, field emitter, and supercapacitor. NaX zeolite with a superior ability of ion exchange and adsorption capacity was incorporated with the carbonized PANI. The LOD obtained by the carbonized PANI–NaX zeolite electrode was way better than the pure NaX zeolite and carbonized PANI electrodes with values of 1.27 μM , 135 μM , and 94.5 μM , respectively [231].

In addition to PANI, its derivative also has been applied as the sensing material for the detection of hazardous phenolic compounds using an AMP sensor. Poly(2,5-dimethoxyaniline) has been prepared through polymerization in the presence of phenanthrene sulfonic acid. LOD values in the range of 0.07–3.71 mM were exhibited for the targets [232].

Table 6 shows the summaries of PANI and its derivative-based materials incorporated with electrochemical for hazardous phenolic compounds detection.

Table 6. PANI and its derivatives-based materials incorporated with electrochemical sensors for hazardous phenolic compounds detection.

Sensing Materials	Sensor	Hazardous Phenolic Compounds	Linear Range	LOD ¹	Ref.
PANI nanosheets electrode	Cyclovoltammetry	Ph	20–80 μ M	4.43 μ M	[222]
<i>Trametes versicolor</i> –PANI thick film electrode	Amperometry	Ph	0.4–6 μ M	-	[223]
<i>Aspergillus niger</i> –PANI thick film electrode			0.4–4 μ M		
<i>Agaricus bisporus</i> –PANI thick film electrode			1–10 μ M		
PANI–laccase–indium tin oxide electrode	Amperometry	Ph	0.5–4.5 μ M	-	[224]
PANI–tyrosinase–platinum electrode	Amperometry	Ph	0.04–25 μ M	10 nM	[225]
PANI–polyacrylonitrile–tyrosinase–platinum electrode	Amperometry	Ph	0.1–75 μ M	-	[226]
PANI–ionic liquid–carbon nanofiber–tyrosinase–glassy carbon electrode	Amperometry	Ph	0.4 nM–1.9 μ M	0.1 nM	[227]
PANI–activated carbon–tyrosinase–carbon paste electrode	Amperometry	Ph	1–50 μ M	0.5 μ M	[228]
Sulfonated PANI–chitosan–tyrosinase–glassy carbon electrode	Voltammetry	Ph	3.5–200 nM 200–2000 nM	0.8 nM	[229]
4-NP imprinted–PANI–polyvinyl sulfonic acid–indium tin oxide electrode	Cyclic voltammetry	4-NP	-	1 μ M	[230]
NaX/carbonized–PANI	Cyclic voltammetry	4-NP	100 μ M–1 mM	1.27 μ M	[231]
Poly(2,5-dimethoxyaniline)–phenanthrene sulfonic acid–platinum electrode	Amperometry	Ph	-	2.09 mM	[232]
		2,4-DCP		2.53 mM	
		2,4,6-TCP		0.07 mM	
		PCP		0.61 mM	
		2,4-NP		0.63 mM	
		2,4-DMP		3.71 mM	

¹ where LOD is limit of detection. 2,4-DCP: 2,4-dichlorophenol, 2,4-DMP: 2,4-dimethylphenol, 2,4-DNP: 2,4-dinitrophenol, 2,4,6-TCP: 2,4,6-trichlorophenol, 4-NP: 4-nitrophenol, PANI: polyaniline, PCP: pentachlorophenol, Ph: phenol.

3.1.3. Poly(3,4-ethylenedioxythiophene)

Poly(3,4-ethylenedioxythiophene) (PEDOT) also has received a lot of attention in the field of sensors as it has high environmental stability, excellent electrical conductivity, and good film-forming properties. An AMP sensor for Ph has been reported based on the immobilization of Tyr on the surface of PEDOT-modified GCE. The linear response spanned the Ph concentration up to 25 μM and gave an LOD of 50 nM [233].

In order to improve the repeatability of sensors, some researchers have modified the PEDOT with a surfactant, poly(sodium-4-styrenesulfonate) (PSS). An LOD of 10 μM with a broad linear response from 10 to 531 μM was obtained for AMP sensing of Ph using PEDOT-PSS-modified Pt electrode. The sensor also showed a good repeatability and reproducibility [234].

PEDOT-PSS also has been used for the chronoamperometric detection of 2-NP and 4-NP. The current response was directly dependent on the concentration of 2-NP and 4-NP up to 80 μM . A slightly lower LOD of 4.51 μM was obtained for 4-NP compared to 2-NP with 4.55 μM . In addition, this sensor was highly selective toward 2-NP and 4-NP in the presence of some ions and organic compounds [235].

Several works based on the incorporation of PEDOT with single-walled carbon nanotubes (SWCNTs) have been conducted, as the SWCNTs are able to facilitate the electron transfer processes that consequently will enhance the mechanical and electrical properties of PEDOT. As the PEDOT-SWCNTs were immobilized on GCE for the AMP detection of Ph, 2,4-DCP, 2,4,6-TCP, and PCP, LOD, and linear responses of 0.094 μM and 0.1–260 μM , 0.39 μM and 0.4–120 μM , 0.3 μM and 1–90 μM , and 0.33 μM and 2–110 μM were obtained, respectively [236].

On the other hand, the SWCNTs-PEDOT composite also has been deposited on the surface of screen-printed carbon electrode. In order to prevent overoxidation of the polymer film, the CV method was used to polymerize the 3,4-ethylenedioxythiophene on the electrode. An LOD of 0.38 μM and two parts of linear response between 0.6–100 μM and 200–600 μM were obtained for the voltammetric sensing of Ph using the modified electrode. Furthermore, the detection of 2,4-DCP obtained linear responses over 0.5–60 μM and 50–300 μM ; meanwhile, for 2,4,6-TCP, it was linear in the range of 0.4–100 μM and 220–500 μM . Both the detection of 2,4-DCP and 2,4,6-TCP achieved an LOD of 0.16 μM [237].

Next, another voltammetric sensor was successfully fabricated for 2,4-DCP sensing. It was based on the immobilization of PEDOT and MIP on the surface of a carbon fiber paper electrode. The peak current increased as the 2,4-DCP concentration increased from 0.21 to 300 nM, and a low LOD was obtained with a value of 0.07 nM. An excellent selectivity toward 2,4-DCP also can be observed [238].

3.2. Extraction Methods with Chromatographic Analysis

3.2.1. Polypyrrole

Due to some superiorities such as good environmental stability, easy to prepare, and low volumes of solvent required for the removal of target analytes, PPy have received considerable attention in the extraction of compounds. PPy has been used as a sorbent for the SPE of pollutants followed by GC-FID and GC-MS detection. It was used for the extraction of a real sample that revealed the LOD of 1.25 nM, 0.58 nM, 0.21 nM, and 75.97 pM for Ph, 2-CP, 2,4-DCP, and 2,4,6-TCP, respectively [239].

Another work also has reported PPy as a sorbent, but this time, the SPE system was used with reversed-phase liquid chromatography-UV detection. The obtained LODs for Ph, 2-CP, 2,4-DCP, and 2,4,6-TCP in double-distilled water were 0.74 nM, 0.31 nM, 61.35 pM, and 0.2 nM, respectively [240].

PPy and Fe_2O_3 nanoparticles have been incorporated as a magnetic sorbent for the extraction of 2-NP, 4-NP, and 2,4-DNP using the MSPE method followed by HPLC-UV detection. In the presence of the nanoparticles, greater extraction capacity can be achieved as it has a high specific surface area-to-volume ratio. The sensor exhibited linearity ranges

of 7.2–718.9 nM, 5.4–718.9 nM, and 5.4–543.2 nM, and LOD of 2.88 nM, 2.16 nM, and 2.17 nM for 2-NP, 4-NP, and 2,4-DNP, respectively [241].

On the other hand, PPy–montmorillonite clay was developed as the fiber coating of the HS-SPME-GC-MS method. Both the conducting polymer and clay exhibited strong interfacial interactions that consequently will lead to the improvement of thermal and mechanical stability. This work gave a linear response from 0.1 to 1 μM for Ph and 0.01 to 1 μM for both 2,4-DCP and 2,4,6-TCP. LOD values of 0.014 μM , 1 nM, and 0.53 nM were obtained for Ph, 2,4-DCP, and 2,4,6-TCP, respectively [242].

3.2.2. Polyaniline and Its Derivatives

In addition to PPy, PANI and its derivative have attracted remarkable attention among researchers as extraction materials due to some reasons such as hydrophilic property, good environmental stability, and a large benzene ring system that will be a huge benefit when interacting with aromatic compounds. One work has utilized PANI as the sorbent for the SPE of 2-CP, 2,4-DCP, 2,4,6-TCP, and PCP from aqueous samples followed by GC-electron-capture (ECD) and FID. The LOD found for the chlorophenols were in the range of 11 to 855 pM [243]. On the other hand, as poly-N-methylaniline was used as the sorbent, lower LOD values in the range of 3.75 to 311 pM were obtained for the chlorophenols. This might be due to the presence of a methyl group on its nitrogen atom that helps to give better recovery for the extraction of the analytes [244].

A fiber coating for Ph, 2-CP, 2,4-DCP, 2,4,6-TCP, and PCP extraction using SPME was prepared based on the electrodeposition of PANI on the surface of Pt wire. Then, it was detected using a GC-FID detector that revealed the linearity and LOD for Ph, 2-CP, 2,4-DCP, 2,4,6-TCP, and PCP were 2.66–53.13 μM and 0.44 μM , 0.39–38.89 μM and 18.67 nM, 0.31–30.67 μM and 22.7 nM, 0.25–25.32 μM and 6.58 nM, and 0.09–18.77 μM and 2.59 nM, respectively [245].

PANI-coated Pt wire also has been used for the extraction of phenolic compounds using HS-SPME coupled to GC-FID. Better performance was observed for 2,4-DMP with an LOD of 10.64 nM and linearity within 0.08–40.93 μM ; meanwhile, 0.14 μM LOD and 0.1–53.13 μM linear response were obtained for Ph [246].

Then, the previous work was improved by immobilizing the PANI together with MWCNTs on the Pt wire. Using an HS-SPME-GC-FID detector, it exhibited low LOD values of 14.7 pM, 6.44 pM, and 67 pM for 2-CP, 2,4-DCP, and 2-NP, respectively. A broad linear response was also observed for each of the analytes between 0.39–777.85 nM, 0.15–214.72 nM, and 0.36–251.6 nM, respectively. The good compatibility between PANI and MWCNTs have led to excellent reusability of the fiber, as the extraction efficiency does not noticeably decrease even after undergoing 216 adsorption/desorption process cycles [247].

Next, carbon-coated Fe_3O_4 magnetic microspheres ($\text{Fe}_3\text{O}_4@\text{C}$) and PANI were synthesized using hydrothermal reactions that will be used as a magnetic adsorbent to extract phenolic compounds using the MSPE-GC-MS procedure. The developed sensor produced a linear range from 0.05 to 2.13 μM for Ph, 0.06 to 1.23 μM for 2,4-DCP, and 18.77 to 750.92 nM for PCP, respectively. The LOD was found out to be at 23 nM, 34 nM, and 12 nM for Ph, 2,4-DCP, and PCP, respectively [248].

PANI has been added to a carbon nanotubes–magnetite nanoparticles composite as the preparation of a fiber coating for HS-SPME of Ph and 2,4,6-TCP. A calibration linearity in the range of 0.001 until 1 μM with an LOD of 0.74 nM was obtained for the extraction of Ph coupled with GC-MS. 2,4,6-TCP, on the other hand, exhibited a wider linear response between 0.05 nM and 2.53 μM and an LOD of 0.1 nM. These great results might be attributed to the enhancement of sorption capability due to the successful interactions between PANI, carbon nanotubes, and magnetite nanoparticles with the target compounds [249].

4. Graphene and Conducting Polymers-Based Composite Materials Incorporated with Various Sensors for Detection of Hazardous Phenolic Compounds

4.1. Electrochemical Sensors

Polycarbazole (PCZ) polymer, Gr, and nitrogen have been incorporated together on GCE to be employed as a CV sensor for 4-NP. The comparison between the proposed PCZ/nitrogen-doped Gr-GCE with other electrodes (bare GCE, RGO-GCE, PCZ-GCE, and nitrogen-doped Gr-GCE) showed that the PCZ/nitrogen-doped Gr-GCE has the most excellent electrochemical catalytic activity toward 4-NP. This is owing to the good catalytic ability of nitrogen atoms that are able to improve the electric properties of Gr and the good synergistic effect between PCZ and nitrogen-doped Gr. The peak current was directly proportional to the concentration of 4-NP in the range of 0.8 to 20 μM , and an LOD of 0.062 μM was obtained [250].

Another CV sensor for the detection of 4-NP was prepared by the synthesis of PANI in GO dispersion in the presence of 4-NP for the fabrication of MIP. The application of MIP in the development of sensors is outstanding owing to its high specificity and great durability against harsh chemical environments. The response was linear to the 4-NP from 0.06 to 1.4 mM, and an LOD of 20 μM was obtained [251].

In order to improve the sensitivity of a DPV sensor for 4-NP sensing, PANI has been reinforced with interconnected and porous hybrid GO–iron tungsten nitride nanoflakes. As a result, the electrocatalytic performance of the PANI–GO–iron tungsten nitride-modified GCE was better compared to PANI-modified GCE. Both oxidation and reduction signals increased when the 4-NP concentration increased from 0.03–3 μM and 0.01–4 μM , respectively. Excellent LOD values were also exhibited in which the LOD for the oxidation peak current and reduction peak current were 5.2 nM and 2.4 nM, respectively [252].

Another DPV sensor was developed by drop coating a mixture of partially RGO–PANI on the surface of GCE, but this time for the detection of Ph. As both RGO and PANI have good electrical conductivity and electrochemical activity, the combination of them resulted in better electrochemical properties. The current response was linear to the Ph concentration over 0.01–10 μM with a correlation coefficient of 0.9922. The LOD was calculated to be 4.5 nM [253].

A work has reported a SWV sensor for 2,4-DCP based on the combination of Gr and PANI that have outstanding electroanalytic activities toward an analyte with diamond, which is an anti-passivating agent that has a high resistance to fouling, on the surface of GCE. The oxidation peaks showed a linear relationship to the analyte concentration from 5 to 80 μM , and the calculated LOD was 0.25 μM [254].

On the other hand, Gr and PANI also have been used in the development of an AMP sensor for 2-NP. The Gr and PANI were incorporated with cerium tungstate on the surface of GCE. The sensor that possesses some excellent characteristics including non-toxic, huge surface area, chemically stable, and good absorption capability gave a wide linearity between 1 nM and 1 mM and an LOD as low as 0.87 nM. In addition, this sensor gave a great selectivity toward 2-NP when tested with several interferents [255].

4.2. Extraction Methods with Chromatographic Analysis

PPy has been modified with Gr to develop a new fiber coating for the SPME of Ph and 2,4-DCP followed by a GC-FID detector. A wider linear response of 0.53–10.63 μM with an LOD of 0.48 μM was obtained for Ph; meanwhile, a lower LOD of 0.025 μM with a linearity between 0.061 and 6.13 μM was estimated for 2,4-DCP. In addition, the extraction efficiency of the PPy-G fiber for 2,4-DCP was way higher compared to Ppy-GO fiber, as it has better hydrophobicity [256].

4.3. Optical Sensors

A colorimetric sensor was successfully fabricated for the detection of Ph by enhancing the enzyme-like catalytic activity of Cu_8S_5 nanoparticles with the modification of the

nanoparticles with PPy and RGO. A broad linear response from 0 to 200 μM and an LOD of 1.78 μM were obtained [257].

5. Future Perspectives of the Study

To date, overwhelming studies for the fabrication of sensors for the detection of hazardous phenolic compounds have been carried out all around the globe due to the potential health effects that they could bring. There has been a vigorous competition among researchers to develop a high sensitivity sensor with the ability to detect the target analytes' concentration as low as possible. The main key to improve the performance of the sensor is by modifying the sensor with highly promising materials. Thus, graphene and conducting polymers-based materials have risen in popularity for the fabrication of sensors due to their superior properties.

As we can see, electrochemical sensors were widely utilized in the detection of the hazardous phenolic compounds followed by the extraction methods with chromatographic analysis and optical methods. As these sensors experienced several drawbacks such as poor selectivity, low sensitivity, and low reusability, the incorporation of the graphene and conducting polymers-based materials with these sensors can be a help to overcome the disadvantages [258–260].

In addition, various combinations of materials with the graphene-based materials and conducting polymers have been discussed in this article. Some of the support materials play a huge role in further improving the sensing properties of the fabricated sensors, and some might be decreasing the efficiency of the sensors for the detection of hazardous phenolic compounds.

In conclusion, this review can be a great reference for researchers for the development of new technology in sensing hazardous phenolic compounds. The new incorporation of materials with sensors and new combinations of materials with graphene-based materials and conducting polymers can be developed. A more sensitive and selective sensor with good stability, reusability, and reproducibility can be invented as well.

6. Conclusions

The trends in the graphene and conducting polymers-based materials incorporated into various sensors for the detection of hazardous phenolic compounds have been successfully reviewed in this paper. Furthermore, this article also reviewed the graphene and conducting polymers-based composite materials in sensors for the hazardous phenolic compounds. To date, a lot of sensors that incorporated graphene and conducting polymers-based materials have been introduced due to their promising and convincing properties, and this trend is expected to continue to expand more in the future.

Author Contributions: Conceptualization, H.S.H., Y.W.F., N.A.S.O. and N.I.M.F.; writing—original draft preparation, H.S.H. and N.A.S.O.; writing—review and editing, H.S.H. and N.A.S.O.; visualization, H.S.H. and N.I.M.F.; supervision, Y.W.F. All authors have read and agreed to the published version of the manuscript.

Funding: This research was funded by Ministry of Education Malaysia through the Fundamental Research Grant Scheme (FRGS) (FRGS/1/2019/STG02/UPM/02/1) and Putra Grant Universiti Putra Malaysia.

Institutional Review Board Statement: Not applicable.

Informed Consent Statement: Not applicable.

Data Availability Statement: Data sharing is not applicable in this article.

Conflicts of Interest: The authors declare no conflict of interest.

References

1. Gami, A.A.; Shukor, M.Y.; Khalil, K.A.; Dahalan, F.A.; Khalid, A.; Ahmad, S.A. Phenol and its toxicity. *J. Environ. Microbiol. Toxicol.* **2014**, *2*, 11–24.
2. Bohdziewicz, J.; Kamińska, G.; Tytła, M. The removal of phenols from wastewater through sorption on the removal of phenols from wastewater through sorption on activated carbon. *Archit. Civ. Eng. Environ.* **2012**, *2*, 89–94.
3. Kafi, A.K.M.; Chen, A. A novel amperometric biosensor for the detection of nitrophenol. *Talanta* **2009**, *79*, 97–102. [[CrossRef](#)]
4. Belekbir, S.; El Azzouzi, M.; El Hamidi, A.; Rodríguez-Lorenzo, J.A.; Santaballa, L.; Canle, M. Improved photocatalyzed degradation of phenol, as a model pollutant, over metal-impregnated nanosized TiO₂. *Nanomaterials* **2020**, *10*, 996. [[CrossRef](#)]
5. Guan, H.; Liu, X.; Wang, W. Encapsulation of tyrosinase within liposome bioreactors for developing an amperometric phenolic compounds biosensor. *J. Solid State Electrochem.* **2013**, *17*, 2887–2893. [[CrossRef](#)]
6. Abdullah, J.; Ahmad, M.; Karupiah, N.; Heng, L.Y.; Sidek, H. Immobilization of tyrosinase in chitosan film for an optical detection of phenol. *Sens. Actuators B* **2006**, *114*, 604–609. [[CrossRef](#)]
7. Wen, Y.; Li, R.; Liu, J.; Zhang, X.; Wang, P.; Zhang, X.; Zhou, B.; Li, H.; Wang, J.; Li, Z.; et al. Promotion effect of Zn on 2D bimetallic NiZn metal organic framework nanosheets for tyrosinase immobilization and ultrasensitive detection of phenol. *Anal. Chim. Acta* **2020**, *1127*, 131–139. [[CrossRef](#)]
8. Jiang, L.; Santiago, I.; Foord, J. Nanocarbon and nanodiamond for high performance phenolics sensing. *Commun. Chem.* **2018**, *1*, 43. [[CrossRef](#)]
9. U.S. Department of Health and Human Services. *Toxicological Profile for Asbestos*; Update; Agency for Toxic Substances and Disease Registry: Atlanta, GA, USA, 1999.
10. Mu'azu, N.D.; Jarrah, N.; Zubair, M.; Alagha, O. Removal of phenolic compounds from water using sewage sludge-based activated carbon adsorption: A review. *Int. J. Environ. Res. Public Health* **2017**, *14*, 1094. [[CrossRef](#)]
11. Raza, W.; Lee, J.; Raza, N.; Luo, Y.; Kim, K.-H.; Yang, J. Removal of phenolic compounds from industrial waste water based on membrane-based technologies. *J. Ind. Eng. Chem.* **2019**, *71*, 1–18. [[CrossRef](#)]
12. Boruah, P.K.; Sharma, B.; Karbhal, I.; Shelke, M.V.; Das, M.R. Ammonia-modified graphene sheets decorated with magnetic Fe₃O₄ nanoparticles for the photocatalytic and photo-Fenton degradation of phenolic compounds under sunlight irradiation. *J. Hazard. Mater.* **2017**, *325*, 90–100. [[CrossRef](#)]
13. Shandilya, P.; Mittal, D.; Soni, M.; Raizada, P.; Lim, J.-H.; Jeong, D.Y.; Dewedi, R.P.; Saini, A.K.; Singh, P. Islanding of EuVO₄ on high-dispersed fluorine doped few layered graphene sheets for efficient photocatalytic mineralization of phenolic compounds and bacterial disinfection. *J. Taiwan Inst. Chem. Eng.* **2018**, *93*, 528–542. [[CrossRef](#)]
14. Meijiao, L.; Jing, L.; XuYu, Y.; ChangAn, Z.; Jia, Y.; Hao, H.; XianBao, W. Applications of graphene-based materials in environmental protection and detection. *Mol. Mater. Devices* **2013**, *58*, 2698–2710.
15. Hashim, H.S.; Fen, Y.W.; Omar, N.A.S.; Daniyal, W.M.E.M.M.; Saleviter, S.; Abdullah, J. Structural, optical and potential sensing properties of tyrosinase immobilized graphene oxide thin film on gold surface. *Optik* **2020**, *212*, 164786. [[CrossRef](#)]
16. Nurrohman, D.T.; Chiu, N.-F. A review of graphene-based surface plasmon resonance and surface-enhanced raman scattering biosensors: Current status and future prospects. *Nanomaterials* **2021**, *11*, 216. [[CrossRef](#)]
17. Popov, A.; Aukstojyte, R.; Gaidukevic, J.; Lisyte, V.; Kausaite-Minkstimiene, A.; Barkauskas, J.; Ramanaviciene, A. Reduced graphene oxide and polyaniline nanofibers nanocomposite for the development of an amperometric glucose biosensor. *Sensors* **2021**, *21*, 948. [[CrossRef](#)]
18. Huang, X.; Yin, Z.; Wu, S.; Qi, X.; He, Q.; Zhang, Q.; Yan, Q.; Boey, F.; Zhang, H. Graphene-based materials: Synthesis, characterization, properties, and applications. *Small* **2011**, *7*, 1876–1902. [[CrossRef](#)]
19. Baig, N.; Kawde, A.N. A novel, fast and cost effective graphene-modified graphite pencil electrode for trace quantification of l-tyrosine. *Anal. Methods* **2015**, *7*, 9535–9541. [[CrossRef](#)]
20. Omar, N.A.S.; Fen, Y.W.; Abdullah, J.; Kamil, Y.M.; Daniyal, W.M.E.M.M.; Sadrolhosseini, A.R.; Mahdi, M.A. Sensitive detection of dengue virus type 2 E-proteins signals using self-assembled monolayers/reduced graphene oxide-PAMAM dendrimer thin film-SPR optical sensor. *Sci. Rep.* **2020**, *10*, 1–15. [[CrossRef](#)]
21. Baig, N.; Saleh, T.A. Electrodes modified with 3D graphene composites: A review on methods for preparation, properties and sensing applications. *Microchim. Acta* **2018**, *2*, 1–21. [[CrossRef](#)]
22. Sun, H.; Wu, L.; Wei, W.; Qu, X. Recent advances in graphene quantum dots for sensing. *Mater. Today* **2013**, *16*, 433–442. [[CrossRef](#)]
23. Zhang, B.; Zhao, R.; Sun, D.; Li, Y.; Wu, T. Sustainable fabrication of graphene oxide/manganese oxide composites for removing phenolic compounds by adsorption-oxidation process. *J. Clean. Prod.* **2019**, *215*, 165–174. [[CrossRef](#)]
24. Abdolmaleki, A.; Mahmoudian, M. Use of biomass sericin as matrices in functionalized graphene/sericin nanocomposites for the removal of phenolic compounds. *Heliyon* **2020**, *6*, e04955. [[CrossRef](#)] [[PubMed](#)]
25. Park, J.M.; Kim, C.M.; Jhung, S.H. Melamine/polyaniline-derived carbons with record-high adsorption capacities for effective removal of phenolic compounds from water. *Chem. Eng. J.* **2020**, 127627. [[CrossRef](#)]
26. Majumdar, S.; Nath, J.; Mahanta, D. Surface modified polypyrrole for the efficient removal of phenolic compounds from aqueous medium. *J. Environ. Chem. Eng.* **2018**, *6*, 2588–2596. [[CrossRef](#)]
27. Tuncagil, S.; Varis, S.; Toppare, L. Design of a biosensor based on 1-(4-nitrophenyl)-2,5-di(2-thienyl)-1H pyrrole. *J. Mol. Catal. B Enzym.* **2010**, *64*, 195–199. [[CrossRef](#)]

28. Abdi, M.M.; Abdullah, L.C.; Sadrolhosseini, A.R.; Yunus, W.M.M.; Moxsin, M.M.; Tahir, P.M. Surface plasmon resonance sensing detection of mercury and lead ions based on conducting polymer composite. *PLoS ONE* **2011**, *6*, e24578. [[CrossRef](#)]
29. Ramanavicius, S.; Ramanavicius, A. Charge transfer and biocompatibility aspects in conducting polymer-based enzymatic biosensors and biofuel cells. *Nanomaterials* **2021**, *11*, 371. [[CrossRef](#)] [[PubMed](#)]
30. Naveen, M.H.; Gurudatt, N.G.; Shim, Y.-B. Applications of conducting polymer composites to electrochemical sensors: A review. *Appl. Mater. Today* **2017**, *9*, 419–433. [[CrossRef](#)]
31. Sulak, M.T.; Erhan, E.; Keskinler, B.; Yilmaz, F.; Celik, A. Development of amperometric biosensor for phenolic compounds using a modified electrode with poly(GMA-co-MTM) and laccase. *Sens. Lett.* **2010**, *8*, 1–6. [[CrossRef](#)]
32. Zhao, Y.; Cao, L.; Li, L.; Cheng, W.; Xu, L.; Ping, X.; Pan, L.; Shi, Y. Conducting polymers and their applications in diabetes management. *Sensors* **2016**, *16*, 1787. [[CrossRef](#)]
33. Gurunathan, K.; Amalnerkar, D.P.; Trivedi, D.C. Synthesis and characterization of conducting polymer composite (PAN/TiO₂) for cathode material in rechargeable battery. *Mater. Lett.* **2003**, *57*, 1642–1648. [[CrossRef](#)]
34. Coskun, Y.; Cirpan, A.; Toppare, L. Conducting polymers of terephthalic acid bis-(2-thiophen-3-yl-ethyl) ester and their electrochromic properties. *Polymer* **2004**, *45*, 4989–4995. [[CrossRef](#)]
35. Lee, A.S.; Peteu, S.F.; Ly, J.V.; Requicha, A.A.G.; Thompson, M.E.; Zhou, C. Actuation of polypyrrole nanowires. *Nanotechnology* **2008**, *19*, 165501. [[CrossRef](#)] [[PubMed](#)]
36. Otero, T.F.; Sanchez, J.J.; Martinez, J.G. Biomimetic dual sensing-actuators based on conducting polymers. Galvanostatic theoretical model for actuators sensing temperature. *J. Phys. Chem. B* **2012**, *116*, 5279–5290. [[CrossRef](#)]
37. Mi, H.; Zhang, X.; Ye, X.; Yang, S. Preparation and enhanced capacitance of core-shell polypyrrole/polyaniline composite electrode for supercapacitors. *J. Power Sources* **2008**, *176*, 403–409. [[CrossRef](#)]
38. Omar, N.A.S.; Fen, Y.W.; Saleviter, S.; Daniyal, W.M.E.M.M.; Anas, N.A.A.; Ramdzan, N.S.M.; Roshidi, M.D.A. Development of a graphene-based surface plasmon resonance optical sensor chip for potential biomedical application. *Materials* **2019**, *12*, 1928. [[CrossRef](#)]
39. Daniyal, W.M.E.M.M.; Fen, Y.W.; Abdullah, J.; Sadrolhosseini, A.R.; Saleviter, S.; Omar, N.A.S. Label-free optical spectroscopy for characterizing binding properties of highly sensitive nanocrystalline cellulose-graphene oxide based nanocomposite towards nickel ion. *Spectrochim. Acta Part A* **2019**, *212*, 25–31. [[CrossRef](#)]
40. Ramdzan, N.S.M.; Fen, Y.W.; Omar, N.A.S.; Anas, N.A.A.; Liew, J.Y.C.; Daniyal, W.M.E.M.M.; Hashim, H.S. Detection of mercury ion using surface plasmon resonance spectroscopy based on nanocrystalline cellulose/poly(3,4-ethylenedioxythiophene) thin film. *Measurement* **2021**, *182*, 109728. [[CrossRef](#)]
41. Coros, M.; Pruneanu, S.; Staden, R.-I.S. Review—Recent progress in the graphene-based electrochemical sensors and biosensors. *J. Electrochem. Soc.* **2020**, *167*, 037528. [[CrossRef](#)]
42. Papageorgiou, D.G.; Kinloch, I.A.; Young, R.J. Mechanical properties of graphene and graphene-based nanocomposites. *Prog. Mater. Sci.* **2017**, *90*, 75–127. [[CrossRef](#)]
43. Pumera, M.; Ambrosi, A.; Bonanni, A.; Chng, E.L.K.; Poh, H.L. Graphene for electrochemical sensing and biosensing. *TrAC-Trends Anal. Chem.* **2010**, *29*, 954–965. [[CrossRef](#)]
44. Ma, H.; Wu, D.; Cui, Z.; Li, Y.; Zhang, Y.; Du, B.; Wei, Q. Graphene-based optical and electrochemical biosensors: A review. *Anal. Lett.* **2013**, *46*, 1–17. [[CrossRef](#)]
45. Brownson, D.A.C.; Banks, C.E. Graphene electrochemistry: An overview of potential applications. *Analyst* **2010**, *135*, 2768–2778. [[CrossRef](#)] [[PubMed](#)]
46. Rahman, M.A.; Kumar, P.; Park, D.-S.; Shim, Y.-B. Electrochemical sensors based on organic conjugated polymers. *Sensors* **2008**, *8*, 118–141. [[CrossRef](#)]
47. Das, T.K.; Prusty, S. Review on conducting polymers and their applications. *Polym.-Plast. Technol. Eng.* **2012**, *51*, 1487–1500. [[CrossRef](#)]
48. Gupta, N.; Sharma, S.; Mir, I.A.; Kumar, D. Advances in sensors based on conducting polymers. *J. Sci. Ind. Res.* **2006**, *65*, 549–557.
49. Ates, M. A review study of (bio)sensor systems based on conducting polymers. *Mater. Sci. Eng. C* **2013**, *33*, 1853–1859. [[CrossRef](#)]
50. Krampa, F.D.; Aniweh, Y.; Awandare, G.A.; Kanyong, P. A disposable amperometric sensor based on high-performance PEDOT:PSS/ionic liquid nanocomposite thin film-modified screen-printed electrode for the analysis of catechol in natural water samples. *Sensors* **2017**, *17*, 1716. [[CrossRef](#)]
51. Liu, T.; Fu, B.; Chen, J.; Yan, Z.; Li, K. A non-enzymatic electrochemical sensor for detection of sialic acid based on a porphyrin/graphene oxide modified electrode via indicator displacement assay. *Electrochim. Acta* **2018**, *269*, 136–143. [[CrossRef](#)]
52. Capannesi, C.; Palchetti, I.; Mascini, M.; Parenti, A. Electrochemical sensor and biosensor for polyphenols detection in olive oils. *Food Chem.* **2000**, *71*, 553–562. [[CrossRef](#)]
53. Fang, Y.; Bullock, H.; Lee, S.A.; Sekar, N.; Eiteman, M.A.; Whitman, W.B.; Ramasamy, R.P. Detection of methyl salicylate using bi-enzyme electrochemical sensor consisting salicylate hydroxylase and tyrosinase. *Biosens. Bioelectron.* **2016**, *85*, 603–610. [[CrossRef](#)] [[PubMed](#)]
54. Terán-Alcocer, Á.; Bravo-Plascencia, F.; Cevallos-Morillo, C.; Palma-Cando, A. electrochemical sensors based on conducting polymers for the aqueous detection of biologically relevant molecules. *Nanomaterials* **2021**, *11*, 252. [[CrossRef](#)] [[PubMed](#)]
55. Bounegru, A.V.; Apetrei, C. Development of a novel electrochemical biosensor based on carbon nanofibers-gold nanoparticles-tyrosinase for the detection of ferulic acid in cosmetics. *Sensors* **2020**, *20*, 6724. [[CrossRef](#)] [[PubMed](#)]

56. Dăscălescu, D.; Apetrei, C. Nanomaterials based electrochemical sensors for serotonin detection: A review. *Chemosensors* **2021**, *9*, 14. [[CrossRef](#)]
57. Coelho, M.K.L.; da Silva, D.N.; Pereira, A.C. Development of electrochemical sensor based on carbonaceous and metal phthalocyanines materials for determination of ethinyl estradiol. *Chemosensors* **2019**, *7*, 32. [[CrossRef](#)]
58. Poole, C.F. New trends in solid-phase extraction. *Trends Anal. Chem.* **2003**, *22*, 362–373. [[CrossRef](#)]
59. Ramdzan, N.S.M.; Fen, Y.W.; Anas, N.A.A.; Omar, N.A.S.; Saleviter, S. Development of biopolymer and conducting polymer-based optical sensors for heavy metal ion detection. *Molecules* **2020**, *25*, 2548. [[CrossRef](#)] [[PubMed](#)]
60. Eddin, F.B.K.; Fen, Y.W. Recent advances in electrochemical and optical sensing of dopamine. *Sensors* **2020**, *20*, 1039. [[CrossRef](#)]
61. Guan, Y.; Liu, L.; Chen, C.; Kang, X.; Xie, Q. Effective immobilization of tyrosinase via enzyme catalytic polymerization of L-DOPA for highly sensitive phenol and atrazine sensing. *Talanta* **2016**, *160*, 125–132. [[CrossRef](#)] [[PubMed](#)]
62. Rodríguez-Delgado, M.M.; Alemán-Nava, G.S.; Rodríguez-Delgado, J.M.; Dieck-Assad, G.; Martínez-Chapa, S.O.; Barceló, D.; Parra, R. Laccase-based biosensors for detection of phenolic compounds. *Trends Anal. Chem.* **2015**, *74*, 21–45. [[CrossRef](#)]
63. Bellido-Milla, D.; Cubillana-Aguilera, L.M.; Kaoutit, M.E.; Hernández-Artiga, M.P.; de Cisneros, J.L.H.-H.; Naranjo-Rodríguez, I.; Palacios-Santander, J.M. Recent advances in graphite powder-based electrodes. *Anal. Bioanal. Chem.* **2013**, *405*, 3525–3539. [[CrossRef](#)]
64. Ortega, F.; Dominguez, E.; Jonsson-Pettersson, G.; Gorton, L. Amperometric biosensor for the determination of phenolic compounds using a tyrosinase graphite electrode in a flow injection system. *J. Biotechnol.* **1993**, *31*, 289–300. [[CrossRef](#)]
65. Liu, F.; Reviejo, A.J.; Pingarron, J.M.; Wang, J. Development of an amperometric for the determination of phenolic in reversed micelles. *Talanta* **1994**, *41*, 455–459. [[CrossRef](#)]
66. Stoytcheva, M.; Zlatev, R.; Gochev, V.; Velkova, Z.; Montero, G.; Beleno, M.T. Amperometric biosensors precision improvement. Application to phenolic pollutants determination. *Electrochim. Acta* **2014**, *147*, 25–30. [[CrossRef](#)]
67. Wang, J.; Reviejo, A.J.; Mannino, S. Organic-phase enzyme electrode for the determination of phenols in olive oils. *Anal. Lett.* **1992**, *25*, 1399–1409. [[CrossRef](#)]
68. Haghghi, B.; Gorton, L.; Ruzgas, T.; Jonsson, L.J. Characterization of graphite electrodes modified with laccase from *Trametes versicolor* and their use for bioelectrochemical monitoring of phenolic compounds in flow injection analysis. *Anal. Chim. Acta* **2003**, *487*, 3–14. [[CrossRef](#)]
69. Jarosz-Wilkolażka, A.; Ruzgas, T.; Gorton, L. Amperometric detection of mono- and diphenols at *Cerrena unicolor* laccase-modified graphite electrode: Correlation between sensitivity and substrate structure. *Talanta* **2005**, *66*, 1219–1224. [[CrossRef](#)]
70. Parellada, J.; Narvaez, A.; Lopez, M.A.; Dominguez, E.; Fernandez, J.J.; Pavlov, V.; Katakis, I. Amperometric immunosensors and enzyme electrodes for environmental applications. *Anal. Chim. Acta* **1998**, *362*, 47–57. [[CrossRef](#)]
71. Kulys, J.; Schmid, R.D. A sensitive enzyme electrode for phenol monitoring. *Anal. Lett.* **1990**, *23*, 589–597. [[CrossRef](#)]
72. Svitel, J.; Miertus, S. Development of tyrosinase-based biosensor and its application for monitoring of bioremediation of phenol and phenolic compounds. *Environ. Sci. Technol.* **1998**, *32*, 828–832. [[CrossRef](#)]
73. Wang, J.; Fang, L.; Lopez, D. Amperometric biosensor for phenols based on a tyrosinase-graphite-epoxy biocomposite. *Analyst* **1994**, *119*, 455–458. [[CrossRef](#)]
74. Onnerfjord, P.; Emneus, J.; Marko-Varga, G.; Gorton, L. Tyrosinase graphite-epoxy based composite electrodes for detection of phenols. *Biosens. Bioelectron.* **1995**, *10*, 607–619. [[CrossRef](#)]
75. Hernandez, S.R.; Kergaravat, S.V.; Pividori, M.I. Enzymatic electrochemical detection coupled to multivariate calibration for the determination of phenolic compounds in environmental samples. *Talanta* **2013**, *106*, 399–407. [[CrossRef](#)] [[PubMed](#)]
76. Munteanu, F.-D.; Lindgren, A.; Emneus, J.; Gorton, L.; Ruzgas, T.; Csoregi, E.; Ciucu, A.; van Huystee, R.B.; Gazaryan, I.G.; Lagrimini, L.M. Bioelectrochemical monitoring of phenols and aromatic amines in flow injection using novel plant peroxidases. *Anal. Chem.* **1998**, *70*, 2596–2600. [[CrossRef](#)] [[PubMed](#)]
77. Serra, B.; Mateo, E.; Pedrero, M.; Reviejo, A.J.; Pingarron, J.M. Graphite-teflon-tyrosinase composite electrodes for the monitoring of phenolic compounds in predominantly non-aqueous media. *Analisis* **1999**, *27*, 592–599. [[CrossRef](#)]
78. Serra, B.; Benito, B.; Agui, L.; Reviejo, A.J.; Pingarron, J.M. Graphite-teflon-peroxidase composite electrochemical biosensors. a tool for the wide detection of phenolic compounds. *Electroanalysis* **2001**, *13*, 693–700. [[CrossRef](#)]
79. Serra, B.; Reviejo, A.J.; Pingarron, J.M. Flow injection amperometric detection of phenolic compounds at enzyme composite biosensors application to their monitoring during industrial waste waters purification processes. *Anal. Lett.* **2003**, *36*, 1965–1986. [[CrossRef](#)]
80. Serra, B.; Reviejo, A.J.; Pingarron, J.M. Composite multienzyme amperometric biosensors for an improved detection of phenolic compounds. *Electroanalysis* **2003**, *15*, 1737–1744. [[CrossRef](#)]
81. Serra, B.; Jimenez, S.; Mena, M.L.; Reviejo, A.J.; Pingarron, J.M. Composite electrochemical biosensors: A comparison of three different electrode matrices for the construction of amperometric tyrosinase biosensors. *Biosens. Bioelectron.* **2002**, *17*, 217–226. [[CrossRef](#)]
82. Carralero-Sanz, V.; Mena, M.L.; Gonzalez-Cortes, A.; Yanez-Sedeno, P.; Pingarron, J.M. Development of a high analytical performance-tyrosinase biosensor based on a composite graphite-Teflon electrode modified with gold nanoparticles. *Biosens. Bioelectron.* **2006**, *22*, 730–736. [[CrossRef](#)]
83. Sapelnikova, S.; Dock, E.; Solna, R.; Skladal, P.; Ruzgas, T.; Emneus, J. Screen-printed multienzyme arrays for use in amperometric batch and flow systems. *Anal. Bioanal. Chem.* **2003**, *376*, 1098–1103. [[CrossRef](#)] [[PubMed](#)]

84. Solna, R.; Dock, E.; Christenson, A.; Winther-Nielsen, M.; Carlsson, C.; Emneus, J.; Ruzgas, T.; Skladal, P. Amperometric screen-printed biosensor arrays with co-immobilised oxidoreductases and cholinesterases. *Anal. Chim. Acta* **2005**, *528*, 9–19. [[CrossRef](#)]
85. Kawde, A.-N.; Aziz, M.A. Porous copper-modified graphite pencil electrode for the amperometric detection of 4-nitrophenol. *Electroanalysis* **2014**, *26*, 1–8. [[CrossRef](#)]
86. Rana, A.; Kawde, A.N. Open-circuit electrochemical polymerization for the sensitive detection of phenols. *Electroanalysis* **2016**, *28*, 898–902. [[CrossRef](#)]
87. Rana, A.; Kawde, A.-N.; Ibrahim, M. Simple and sensitive detection of 4-nitrophenol in real water samples using gold nanoparticles modified pretreated graphite pencil electrode. *J. Electroanal. Chem.* **2018**, *820*, 24–31. [[CrossRef](#)]
88. Shahbakhsh, M.; Noroozifar, M. Poly (dopamine quinone-chromium (III) complex) microspheres as new modifier for simultaneous determination of phenolic compounds. *Biosens. Bioelectron.* **2018**, *102*, 439–448. [[CrossRef](#)]
89. Nissim, R.; Compton, R.G. Introducing absorptive stripping voltammetry: Wide concentration range voltammetric phenol detection. *Analyst* **2014**, *139*, 5911–5918. [[CrossRef](#)] [[PubMed](#)]
90. Wang, X.; Lu, X.; Wu, L.; Chen, J. Direct electrochemical tyrosinase biosensor based on mesoporous carbon and co₃o₄ nanorods for the rapid detection of phenolic pollutants. *ChemElectroChem* **2014**, *1*, 808–816. [[CrossRef](#)]
91. Wang, P.; Xiao, J.; Guo, M.; Xia, Y.; Li, Z.; Jiang, X.; Huang, W. Voltammetric determination of 4-nitrophenol at graphite nanoflakes modified glassy carbon electrode. *J. Electrochem. Soc.* **2015**, *162*, H72–H78. [[CrossRef](#)]
92. Yin, H.Y.; Zheng, Y.F.; Wang, L. Au/CeO₂/g-C₃N₄ nanocomposite modified electrode as electrochemical sensor for the determination of phenol. *J. Nanosci. Nanotechnol.* **2020**, *20*, 5539–5545. [[CrossRef](#)] [[PubMed](#)]
93. Arvinte, A.; Mahosenaho, M.; Pinteala, M.; Sesay, A.-M.; Virtanen, V. Electrochemical oxidation of p-nitrophenol using graphene-modified electrodes, and a comparison to the performance of MWNT-based electrodes. *Microchem. J.* **2011**, *174*, 337–343. [[CrossRef](#)]
94. Shi, J.-J.; Zhu, J.-J. Sono-electrochemical fabrication of Pd-graphene nanocomposite and its application in the determination of chlorophenols. *Electrochim. Acta* **2011**, *56*, 6008–6013. [[CrossRef](#)]
95. Wu, C.; Cheng, Q.; Wu, K. Electrochemical functionalization of N-methyl-2-pyrrolidone-exfoliated graphene nanosheets as highly sensitive analytical platform for phenols. *Anal. Chem.* **2015**, *87*, 3294–3299. [[CrossRef](#)]
96. Hu, F.-T.; Liu, S.-Q. Enhanced effects of surfactant on sensing of phenol on a graphene nano-sheet paste electrode. *Int. J. Electrochem. Sci.* **2012**, *7*, 11338–11350.
97. Hashemnia, S.; Khayat-zadeh, S.; Hashemnia, M. Electrochemical detection of phenolic compounds using composite film of multiwall carbon nanotube/surfactant/tyrosinase on a carbon paste electrode. *J. Solid State Electrochem.* **2012**, *16*, 473–479. [[CrossRef](#)]
98. Li, X.; Shen, J.; Wu, C.; Wu, K. Ball-mill-exfoliated graphene: Tunable electrochemistry and phenol sensing. *Small* **2019**, *15*, 1805567. [[CrossRef](#)]
99. Zhang, Y.; Lu, D.; Ju, T.; Wang, L.; Lin, S.; Zhao, Y.; Wang, C.; He, H.; Du, Y. Biodegradation of phenol using *Bacillus cereus* WJ1 and evaluation of degradation efficiency based on a graphene-modified electrode. *Int. J. Electrochem. Sci.* **2013**, *8*, 504–519.
100. Li, J.; Miao, D.; Yang, R.; Qu, L.; Harrington, P. de B. Synthesis of poly(sodium 4-styrenesulfonate) functionalized graphene/cetyltrimethylammonium bromide (CTAB) nanocomposite and its application in electrochemical oxidation of 2,4-dichlorophenol. *Electrochim. Acta* **2014**, *125*, 1–8. [[CrossRef](#)]
101. Devasenathipathy, R.; Mani, V.; Chen, S.-M.; Manibalan, K.; Huang, S.-T. Determination of 4-nitrophenol at iron phthalocyanine decorated graphene nanosheets film modified electrode. *Int. J. Electrochem. Sci.* **2015**, *10*, 1384–1392.
102. Zhang, W.; Chang, J.; Chen, J.; Xu, F.; Wang, F.; Jiang, K.; Gao, Z. Graphene-Au composite sensor for electrochemical detection of para-nitrophenol. *Res. Chem. Intermed.* **2012**, *38*, 2443–2455. [[CrossRef](#)]
103. Jiao, X.X.; Luo, H.Q.; Li, N.B. Fabrication of graphene-gold nanocomposites by electrochemical co-reduction and their electrocatalytic activity toward 4-nitrophenol oxidation. *J. Electroanal. Chem.* **2013**, *691*, 83–89. [[CrossRef](#)]
104. Deng, P.; Xu, Z.; Li, J. Simultaneous voltammetric determination of 2-nitrophenol and 4-nitrophenol based on an acetylene black paste electrode modified with a graphene-chitosan composite. *Microchim. Acta* **2014**, *181*, 1077–1084. [[CrossRef](#)]
105. Tang, J.; Zhang, L.; Han, G.; Liu, Y.; Tang, W. Graphene-chitosan composite modified electrode for simultaneous detection of nitrophenol isomers. *J. Electrochem. Soc.* **2015**, *162*, 269–274. [[CrossRef](#)]
106. Liu, F.; Piao, Y.; Choi, J.S.; Seo, T.S. Three-dimensional graphene micropillar based electrochemical sensor for phenol detection. *Biosens. Bioelectron.* **2013**, *50*, 387–392. [[CrossRef](#)]
107. Xu, Q.; Li, X.; Zhou, Y.; Wei, H.; Hu, X.-Y.; Wang, Y.; Yang, Z. An enzymatic amplified system for the detection of 2,4-dichlorophenol based on graphene membrane modified electrode. *Anal. Methods* **2012**, *4*, 3429–3435. [[CrossRef](#)]
108. Fartas, F.M.; Abdullah, J.; Yusof, N.A.; Sulaiman, Y.; Saiman, M.I. Biosensor based on tyrosinase immobilized on graphene-decorated gold nanoparticle/chitosan for phenolic detection in aqueous. *Sensors* **2017**, *17*, 1132. [[CrossRef](#)] [[PubMed](#)]
109. Qu, Y.; Ma, M.; Wang, Z.; Zhan, G.; Li, B.; Wang, X.; Fang, H.; Zhang, H.; Li, C. Sensitive amperometric biosensor for phenolic compounds based on graphene-silk peptide/tyrosinase composite nanointerface. *Biosens. Bioelectron.* **2013**, *44*, 85–88. [[CrossRef](#)]
110. Liu, J.; Chen, Y.; Guo, Y.; Yang, F.; Cheng, F. Electrochemical sensor for o-nitrophenol based on β-cyclodextrin functionalized graphene nanosheets. *J. Nanomater.* **2013**, *2013*, 632809. [[CrossRef](#)]

111. Zhu, G.; Qian, J.; Sun, H.; Wu, X.; Wang, K.; Yi, Y. Voltammetric determination of o-chlorophenol using β -cyclodextrin/graphene nanoribbon hybrids modified electrode. *J. Electroanal. Chem.* **2017**, *794*, 126–131. [[CrossRef](#)]
112. Wei, M.; Tian, D.; Liu, S.; Zheng, X.; Duan, S.; Zhou, C. β -cyclodextrin functionalized graphene material: A novel electrochemical sensor for simultaneous determination of 2-chlorophenol and 3-chlorophenol. *Sens. Actuators B* **2014**, *195*, 452–458. [[CrossRef](#)]
113. Gao, J.; Liu, M.; Song, H.; Zhang, S.; Qian, Y.; Li, A. Highly-sensitive electrocatalytic determination for toxic phenols based on coupled cMWCNT/cyclodextrin edge-functionalized graphene composite. *J. Hazard. Mater.* **2016**, *318*, 99–108. [[CrossRef](#)]
114. Liu, W.; Li, C.; Gu, Y.; Tang, L.; Zhang, Z.; Yang, M. One-step synthesis of β -cyclodextrin functionalized graphene/Ag nanocomposite and its application in sensitive determination of 4-nitrophenol. *Electroanalysis* **2013**, *25*, 2367–2376. [[CrossRef](#)]
115. Yang, L.; Zhao, H.; Li, Y.; Li, C.-P. Electrochemical simultaneous determination of hydroquinone and p-nitrophenol based on host-guest molecular recognition capability of dual β -cyclodextrin functionalized Au@graphene nano hybrids. *Sens. Actuators B* **2015**, *207*, 1–8. [[CrossRef](#)]
116. He, Q.; Tian, Y.; Wu, Y.; Liu, J.; Li, G.; Deng, P.; Chen, D. Facile and ultrasensitive determination of 4-nitrophenol based on acetylene black paste and graphene hybrid electrode. *Nanomaterials* **2019**, *9*, 429. [[CrossRef](#)]
117. Bharath, G.; Veeramani, V.; Chen, S.-M.; Madhu, R.; Raja, M.M.; Balamurugan, A.; Mangalaraj, D.; Viswanathana, C.; Ponpandian, N. Edge-carboxylated graphene anchoring magnetite-hydroxyapatite nanocomposite for an efficient 4-nitrophenol sensor. *RSC Adv.* **2015**, *5*, 13392–13401. [[CrossRef](#)]
118. Meng, Z.; Li, M.; Li, C.; Liu, X.; Lei, Z. A sensitive phenol electrochemical sensor based on magnetic oxide/amino-functional graphene nanocomposite. *Int. J. Electrochem. Sci.* **2019**, *14*, 3126–3137. [[CrossRef](#)]
119. Nurdin, M.; Agus, L.; Putra, A.A.M.; Maulidiyah, M.; Arham, Z.; Wibowo, D.; Muzakkar, M.Z.; Umar, A.A. Synthesis and electrochemical performance of graphene-TiO₂-carbon paste nanocomposites electrode in phenol detection. *J. Phys. Chem. Solids* **2019**, *131*, 104–110. [[CrossRef](#)]
120. Wibowo, D.; Sufandy, Y.; Irwan, I.; Azis, T.; Maulidiyah, M.; Nurdin, M. Investigation of nickel slag waste as a modifier on graphene-TiO₂ microstructure for sensing phenolic compound. *J. Mater. Sci. Mater. Electron.* **2020**, *31*, 14375–14383. [[CrossRef](#)]
121. Yin, H.Y.; Zheng, Y.F.; Wang, L. Electrochemical sensor based on Na⁺-doped g-C₃N₄ for detection of phenol. *Bull. Mater. Sci.* **2020**, *43*, 110. [[CrossRef](#)]
122. Daniyal, W.M.E.M.M.; Fen, Y.W.; Abdullah, J.; Saleviter, S.; Omar, N.A.S. Preparation and characterization of hexadecyltrimethylammonium bromide modified nanocrystalline cellulose/graphene oxide composite thin film and its potential in sensing copper ion using surface plasmon resonance technique. *Optik* **2018**, *173*, 71–77. [[CrossRef](#)]
123. Li, J.; Kuang, D.; Feng, Y.; Zhang, F.; Xu, Z.; Liu, M. A graphene oxide-based electrochemical sensor for sensitive determination of 4-nitrophenol. *J. Hazard. Mater.* **2012**, *201–202*, 250–259. [[CrossRef](#)]
124. Liu, Y.; Zhu, L.; Zhang, Y.; Tang, H. Electrochemical sensing of 2,4-dinitrophenol by using composites of graphene oxide with surface molecular imprinted polymer. *Sens. Actuators B* **2012**, *171–172*, 1151–1158. [[CrossRef](#)]
125. Liang, Y.; Yu, L.; Yang, R.; Li, X.; Qu, L.; Li, J. High sensitive and selective graphene oxide/molecularly imprinted polymer electrochemical sensor for 2,4-dichlorophenol in water. *Sens. Actuators B* **2017**, *240*, 1330–1335. [[CrossRef](#)]
126. Arfin, T.; Bushra, R.; Mohammad, F. Electrochemical sensor for the sensitive detection of o-nitrophenol using graphene oxide-poly(ethyleneimine) dendrimer-modified glassy carbon electrode. *Graphene Technol.* **2016**, *1*, 1–15. [[CrossRef](#)]
127. Ragu, S.; Chen, S.-M.; Ranganathan, P.; Rwei, S.-P. Fabrication of a novel nickel-curcumin/graphene oxide nanocomposites for superior electrocatalytic activity toward the detection of toxic p-nitrophenol. *Int. J. Electrochem. Sci.* **2016**, *11*, 9133–9144. [[CrossRef](#)]
128. Zhu, X.; Zhang, K.; Lu, N.; Yuan, X. Simultaneous determination of 2,4,6-trichlorophenol and pentachlorophenol based on poly(Rhodamine B)/graphene oxide/multiwalled carbon nanotubes composite film modified electrode. *Appl. Surf. Sci.* **2016**, *361*, 72–79. [[CrossRef](#)]
129. Gan, T.; Lv, Z.; Sun, J.; Shi, Z.; Liu, Y. Preparation of graphene oxide-wrapped carbon sphere@silver spheres for high performance chlorinated phenols sensor. *J. Hazard. Mater.* **2016**, *302*, 188–197. [[CrossRef](#)]
130. Zhan, T.; Tan, Z.; Tian, X.; Hou, W. Ionic liquid functionalized graphene oxide-Au nanoparticles assembly for fabrication of electrochemical 2,4-dichlorophenol sensor. *Sens. Actuators B* **2017**, *246*, 638–646. [[CrossRef](#)]
131. Arfin, T.; Rangari, S.N. Graphene oxide-ZnO nanocomposite modified electrode for the detection of phenol. *Anal. Methods* **2018**, *10*, 347–358. [[CrossRef](#)]
132. Gan, T.; Wang, Z.; Gao, J.; Sun, J.; Wu, K.; Wang, H.; Liu, Y. Morphology-dependent electrochemical activity of Cu₂O polyhedrons and construction of sensor for simultaneous determination of phenolic compounds with graphene oxide as reinforcement. *Sens. Actuators B* **2019**, *282*, 549–558. [[CrossRef](#)]
133. Singh, S.; Kumar, N.; Meena, V.K.; Kranz, C.; Mishra, S. Impedometric phenol sensing using graphenated electrochip. *Sens. Actuators B* **2016**, *237*, 318–328. [[CrossRef](#)]
134. Wiench, P.; Grzyb, B.; González, Z.; Menéndez, R.; Handke, B.; Gryglewicz, G. pH robust electrochemical detection of 4-nitrophenol on a reduced graphene oxide modified glassy carbon electrode. *J. Electroanal. Chem.* **2017**, *787*, 80–87. [[CrossRef](#)]
135. Rao, H.; Guo, W.; Hou, H.; Wang, H.; Yin, B.; Xue, Z.; Zhao, G. Electroanalytical investigation of p-nitrophenol with dual electroactive groups on a reduced graphene oxide modified glassy carbon electrode. *Int. J. Electrochem. Sci.* **2017**, *12*, 1052–1063. [[CrossRef](#)]

136. Xu, C.; Wang, J.; Wan, L.; Lin, J.; Wang, X. Microwave-assisted covalent modification of graphene nanosheets with hydroxypropyl- β -cyclodextrin and its electrochemical detection of phenolic organic pollutants. *J. Mater. Chem.* **2011**, *21*, 10463–10471. [[CrossRef](#)]
137. Liu, Z.; Ma, X.; Zhang, H.; Lu, W.; Ma, H.; Hou, S. Simultaneous Determination of nitrophenol isomers based on β -cyclodextrin functionalized reduced graphene oxide. *Electroanalysis* **2012**, *24*, 1178–1185. [[CrossRef](#)]
138. Li, C.; Wu, Z.; Yang, H.; Deng, L.; Chen, X. Reduced graphene oxide-cyclodextrin-chitosan electrochemical sensor: Effective and simultaneous determination of o- and p-nitrophenols. *Sens. Actuators B* **2017**, *251*, 446–454. [[CrossRef](#)]
139. Chen, R.; Zhang, Q.; Gu, Y.; Tang, L.; Li, C.; Zhang, Z. One-pot green synthesis of Prussian blue nanocubes decorated reduced graphene oxide using mushroom extract for efficient 4-nitrophenol reduction. *Anal. Chim. Acta* **2014**, *853*, 579–587. [[CrossRef](#)] [[PubMed](#)]
140. Ikhsan, N.I.; Rameshkumar, P.; Huang, N.M. Controlled synthesis of reduced graphene oxide supported silver nanoparticles for selective and sensitive electrochemical detection of 4-nitrophenol. *Electrochim. Acta* **2016**, *192*, 392–399. [[CrossRef](#)]
141. Noor, A.M.; Rameshkumar, P.; Yusoff, N.; Ming, H.N.; Sajab, M.S. Microwave synthesis of reduced graphene oxide decorated with silver nanoparticles for electrochemical determination of 4-nitrophenol. *Ceram. Int.* **2016**, *42*, 18813–18820. [[CrossRef](#)]
142. Wang, L.; Li, X.; Yang, R.; Li, J.-J.; Qu, L.-B. A highly sensitive and selective electrochemical sensor for pentachlorophenol based on reduced graphite oxide-silver nanocomposites. *Food Anal. Methods* **2020**, *13*, 2050–2058. [[CrossRef](#)]
143. Tang, Y.; Huang, R.; Liu, C.; Yang, S.; Lu, Z.; Luo, S. Electrochemical detection of 4-nitrophenol based on a glassy carbon electrode modified with a reduced graphene oxide/Au nanoparticle composite. *Anal. Methods* **2013**, *5*, 5508–5514. [[CrossRef](#)]
144. Liu, F.; Piao, Y.; Choi, K.S.; Seo, T.S. Fabrication of free-standing graphene composite films as electrochemical biosensors. *Carbon N. Y.* **2012**, *50*, 123–133. [[CrossRef](#)]
145. Penu, R.; Obreja, A.C.; Patroi, D.; Diaconu, M.; Radu, G.L. Graphene and gold nanoparticles based reagentless biodevice for phenolic endocrine disruptors monitoring. *Microchem. J.* **2015**, *121*, 130–135. [[CrossRef](#)]
146. Zhang, Y.; Zhang, J.; Wu, H.; Guo, S.; Zhang, J. Glass carbon electrode modified with horseradish peroxidase immobilized on partially reduced graphene oxide for detecting phenolic compounds. *J. Electroanal. Chem.* **2012**, *681*, 49–55. [[CrossRef](#)]
147. Boujakhrou, A.; Jimenez-Falcao, S.; Martínez-Ruiz, P.; Sánchez, A.; Díez, P.; Pingarrón, J.M.; Villalonga, R. Novel reduced graphene oxide-glycol chitosan nanohybrid for the assembly of amperometric enzyme biosensor for phenols. *Analyst* **2016**, *141*, 4162–4169. [[CrossRef](#)]
148. Vilian, A.T.E.; Choe, S.R.; Giribabu, K.; Jang, S.-C.; Roh, C.; Huh, Y.S.; Han, Y.-K. Pd nanospheres decorated reduced graphene oxide with multi-functions: Highly efficient catalytic reduction and ultrasensitive sensing of hazardous 4-nitrophenol pollutant. *J. Hazard. Mater.* **2017**, *333*, 54–62. [[CrossRef](#)] [[PubMed](#)]
149. Zaidi, S.A.; Shin, J.H. A novel and highly sensitive electrochemical monitoring platform for 4-nitrophenol on MnO₂ nanoparticles modified graphene surface. *RSC Adv.* **2015**, *5*, 88996–89002. [[CrossRef](#)]
150. Cheng, Y.; Li, Y.; Li, D.; Zhang, B.; Hao, R.; Sang, S. A sensor for detection of 4-nitrophenol based on a glassy carbon electrode modified with a reduced graphene oxide/Fe₃O₄ nanoparticle composite. *Int. J. Electrochem. Sci.* **2017**, *12*, 7754–7764. [[CrossRef](#)]
151. Sha, R.; Puttapati, S.K.; Srikanth, V.V.; Badhulika, S. Ultra-sensitive phenol sensor based on overcoming surface fouling of reduced graphene oxide-zinc oxide composite electrode. *J. Electroanal. Chem.* **2017**, *785*, 26–32. [[CrossRef](#)]
152. Mohammad, A.; Ahmad, K.; Rajak, R.; Mobin, S.M. Binder free modification of glassy carbon electrode by employing reduced graphene oxide/ZnO composite for voltammetric determination of certain nitroaromatics. *Electroanalysis* **2017**, *29*, 1–10. [[CrossRef](#)]
153. Alam, M.K.; Rahman, M.M.; Abbas, M.; Torati, S.R.; Asiri, A.M.; Kim, D.; Kim, C. Ultra-sensitive 2-nitrophenol detection based on reduced graphene oxide/ZnO nanocomposites. *J. Electroanal. Chem.* **2017**, *788*, 66–73. [[CrossRef](#)]
154. Dutta, S.; Biswas, S.; Maji, R.C.; Saha, R. Environmentally sustainable fabrication of Cu_{1.94}S-rGO composite for dual environmental application: Visible-light-active photocatalyst and room-temperature phenol sensor. *ACS Sustain. Chem. Eng.* **2018**, *6*, 835–845. [[CrossRef](#)]
155. Giribabu, K.; Suresh, R.; Manigandan, R.; Kumar, S.P.; Muthamizh, S.; Munusamy, S.; Narayanan, V. Preparation of nitrogen-doped reduced graphene oxide and its use in a glassy carbon electrode for sensing 4-nitrophenol at nanomolar levels. *Microchim. Acta* **2014**, *181*, 1863–1870. [[CrossRef](#)]
156. Kumar, D.R.; Kesavan, S.; Baynosa, M.L.; Shim, J.J. 3,5-Diamino-1,2,4-triazole@electrochemically reduced graphene oxide film modified electrode for the electrochemical determination of 4-nitrophenol. *Electrochim. Acta* **2017**, *246*, 1131–1140. [[CrossRef](#)]
157. Liu, Y.; Liang, Y.; Yang, R.; Li, J.; Qu, L. A highly sensitive and selective electrochemical sensor based on polydopamine functionalized graphene and molecularly imprinted polymer for the 2,4-dichlorophenol recognition and detection. *Talanta* **2019**, *195*, 691–698. [[CrossRef](#)] [[PubMed](#)]
158. Khan, M.Z.H.; Zhu, J.; Liu, X. Reduced graphene oxide-conjugated urchin-like NiCo₂O₄ nanostructures for individual detection of o-nitro and p-amino phenol. *ACS Omega* **2019**, *4*, 11433–11439. [[CrossRef](#)]
159. Li, Y.; Wang, L.; Zhang, J.; Guo, S. Gold electrode fused with AuNPs/GQDs showing enhanced electrochemical performance for detection of phenolic compounds. *J. Electrochem. Soc.* **2019**, *166*, 1707–1711. [[CrossRef](#)]
160. Liu, Q.; Shi, J.; Zeng, L.; Wang, T.; Cai, Y.; Jiang, G. Evaluation of graphene as an advantageous adsorbent for solid-phase extraction with chlorophenols as model analytes. *J. Chromatogr. A* **2011**, *1218*, 197–204. [[CrossRef](#)]

161. Pan, S.-D.; Zhou, L.-X.; Zhao, Y.-G.; Chen, X.-H.; Shen, H.-Y.; Cai, M.-Q.; Jin, M.-C. Amine-functional magnetic polymer modified graphene oxide as magnetic solid-phase extraction materials combined with liquid chromatography-tandem mass spectrometry for chlorophenols analysis in environmental water. *J. Chromatogr. A* **2014**, *1362*, 34–42. [[CrossRef](#)]
162. Cai, M.-Q.; Su, J.; Hu, J.-Q.; Wang, Q.; Dong, C.-Y.; Pan, S.-D.; Jin, M.-C. Planar graphene oxide-based magnetic ionic liquid nanomaterial for extraction of chlorophenols from environmental water samples coupled with liquid chromatography-tandem mass spectrometry. *J. Chromatogr. A* **2016**, *1459*, 38–46. [[CrossRef](#)] [[PubMed](#)]
163. Chen, X.-H.; Pan, S.-D.; Ye, M.-J.; Li, X.-P.; Zhao, Y.-G.; Jin, M.-C. Magnetic solid-phase extraction based on a triethylenetetramine-functionalized magnetic graphene oxide composite for the detection of ten trace phenolic environmental estrogens in environmental water. *J. Sep. Sci.* **2016**, *39*, 762–768. [[CrossRef](#)]
164. Zhang, R.; Su, P.; Yang, Y. Microwave-assisted preparation of magnetic nanoparticles modified with graphene oxide for the extraction and analysis of phenolic compounds. *J. Sep. Sci.* **2014**, *37*, 3339–3346. [[CrossRef](#)]
165. Abdolmohammad-Zadeh, H.; Zamani, A.; Shamsi, Z. Extraction of four endocrine-disrupting chemicals using a Fe₃O₄/graphene oxide/di-(2-ethylhexyl) phosphoric acid nano-composite, and their quantification by HPLC-UV. *Microchem. J.* **2020**, *157*, 104964. [[CrossRef](#)]
166. Li, F.; Cai, C.; Cheng, J.; Zhou, H.; Ding, K.; Zhang, L. Extraction of endocrine disrupting phenols with iron-ferric oxide core-shell nanowires on graphene oxide nanosheets, followed by their determination by HPLC. *Microchim. Acta* **2015**, *182*, 2503–2511. [[CrossRef](#)]
167. Hou, X.; Yu, H.; Guo, Y.; Liang, X.; Wang, S.; Wang, L.; Liu, X. Polyethylene glycol/graphene oxide coated solid-phase microextraction fiber for analysis of phenols and phthalate esters coupled with gas chromatography. *J. Sep. Sci.* **2015**, *38*, 2700–2707. [[CrossRef](#)]
168. Liu, Y.; Huang, Y.; Chen, G.; Huang, J.; Zheng, J.; Xu, J.; Liu, S.; Qiu, J.; Yin, L.; Ruan, W.; et al. A graphene oxide-based polymer composite coating for highly-efficient solid phase microextraction of phenols. *Anal. Chim. Acta* **2018**, *1015*, 20–26. [[CrossRef](#)]
169. Sun, M.; Bu, Y.; Feng, J.; Luo, C. Graphene oxide reinforced polymeric ionic liquid monolith solid-phase microextraction sorbent for high-performance liquid chromatography analysis of phenolic compounds in aqueous environmental samples. *J. Sep. Sci.* **2016**, *39*, 375–382. [[CrossRef](#)] [[PubMed](#)]
170. Luo, Y.-B.; Zhu, G.-T.; Li, X.-S.; Yuan, B.-F.; Feng, Y.-Q. Facile fabrication of reduced graphene oxide-encapsulated silica: A sorbent for solid-phase extraction. *J. Chromatogr. A* **2013**, *1299*, 10–17. [[CrossRef](#)] [[PubMed](#)]
171. Yang, S.; Liang, J.; Luo, S.; Liu, C.; Tang, Y. Supersensitive detection of chlorinated phenols by multiple amplification electrochemiluminescence sensing based on carbon quantum dots/graphene. *Anal. Chem.* **2013**, *85*, 7720–7725. [[CrossRef](#)] [[PubMed](#)]
172. Luo, S.; Xiao, H.; Yang, S.; Liu, C.; Liang, J.; Tang, Y. Ultrasensitive detection of pentachlorophenol based on enhanced electrochemiluminescence of Au nanoclusters/graphene hybrids. *Sens. Actuators B* **2014**, *194*, 325–331. [[CrossRef](#)]
173. Jiang, D.; Du, X.; Liu, Q.; Zhou, L.; Qian, J.; Wang, K. One-step thermal-treatment route to fabricate well-dispersed ZnO nanocrystals on nitrogen-doped graphene for enhanced electrochemiluminescence and ultrasensitive detection of pentachlorophenol. *ACS Appl. Mater. Interfaces* **2015**, *7*, 3093–3100. [[CrossRef](#)] [[PubMed](#)]
174. Qiu, N.; Liu, Y.; Xiang, M.; Lu, X.; Yang, Q.; Guo, R. A facile and stable colorimetric sensor based on three-dimensional graphene/mesoporous Fe₃O₄ nanohybrid for highly sensitive and selective detection of p-nitrophenol. *Sens. Actuators B* **2018**, *266*, 86–94. [[CrossRef](#)]
175. Hashim, H.S.; Fen, Y.W.; Omar, N.A.S.; Fauzi, N.I.M.; Daniyal, W.M.E.M.M. Recent advances of priority phenolic compounds detection using phenol oxidases-based electrochemical and optical sensors. *Measurement* **2021**, *184*, 109855. [[CrossRef](#)]
176. Daniyal, W.M.E.M.M.; Fen, Y.W.; Fauzi, N.I.M.; Hashim, H.S.; Ramdzan, N.S.M.; Omar, N.A.S. Recent advances in surface plasmon resonance optical sensors for potential application in environmental monitoring. *Sensors Mater.* **2020**, *32*, 4191. [[CrossRef](#)]
177. Ramdzan, N.S.M.; Fen, Y.W.; Omar, N.A.S.; Anas, N.A.A.; Daniyal, W.M.E.M.M.; Saleviter, S.; Zainudin, A.A. Optical and surface plasmon resonance sensing properties for chitosan/carboxyl-functionalized graphene quantum dots thin film. *Optik* **2019**, *178*, 802–812. [[CrossRef](#)]
178. Hashim, H.S.; Fen, Y.W.; Omar, N.A.S.; Abdullah, J.; Daniyal, W.M.E.M.M.; Saleviter, S. Detection of phenol by incorporation of gold modified-enzyme based graphene oxide thin film with surface plasmon resonance technique. *Opt. Express* **2020**, *28*, 9738–9752. [[CrossRef](#)]
179. Deng, Y.; Chang, Q.; Yin, K.; Liu, C.; Wang, Y. A highly stable electrochemiluminescence sensing system of cadmium sulfide nanowires/graphene hybrid for supersensitive detection of pentachlorophenol. *Chem. Phys. Lett.* **2017**, *685*, 157–164. [[CrossRef](#)]
180. Mitra, R.; Saha, A. Reduced graphene oxide based ‘turn-on’ fluorescence sensor for highly reproducible and sensitive detection of small organic pollutants. *ACS Sustain. Chem. Eng.* **2017**, *5*, 604–615. [[CrossRef](#)]
181. Darabdhara, G.; Das, M.R. Dual responsive magnetic Au@Ni nanostructures loaded reduced graphene oxide sheets for colorimetric detection and photocatalytic degradation of toxic phenolic compounds. *J. Hazard. Mater.* **2019**, *368*, 365–377. [[CrossRef](#)]
182. Wang, Y.; Zhao, M.; Hou, C.; Yang, X.; Li, Z.; Meng, Q.; Liang, C. Graphene-based magnetic metal organic framework nanocomposite for sensitive colorimetric detection and facile degradation of phenol. *J. Taiwan Inst. Chem. Eng.* **2019**, *102*, 312–320. [[CrossRef](#)]
183. Anas, N.A.A.; Fen, Y.W.; Omar, N.A.S.; Ramdzan, N.S.M.; Daniyal, W.M.E.M.M.; Saleviter, S.; Zainudin, A.A. Optical properties of chitosan/hydroxyl-functionalized graphene quantum dots thin film for potential optical detection of ferric (III) ion. *Opt. Laser Technol.* **2019**, *120*, 105724. [[CrossRef](#)]

184. Sun, R.; Wang, Y.; Ni, Y.; Kokot, S. Graphene quantum dots and the resonance light scattering technique for trace analysis of phenol in different water samples. *Talanta* **2014**, *125*, 341–346. [[CrossRef](#)]
185. Anh, N.T.N.; Doong, R.-A. One-step synthesis of size-tunable gold@sulfur-doped graphene quantum dot nanocomposites for highly selective and sensitive detection of nanomolar 4-nitrophenol in aqueous solutions with complex matrix. *ACS Appl. Nano Mater.* **2018**, *1*, 2153–2163. [[CrossRef](#)]
186. Zhou, Y.; Qu, Z.-B.; Zeng, Y.; Zhou, T.; Shi, G. A novel composite of graphene quantum dots and molecularly imprinted polymer for fluorescent detection of parantiphenol. *Biosens. Bioelectron.* **2014**, *52*, 317–323. [[CrossRef](#)]
187. Anh, N.T.N.; Chang, P.-Y.; Doong, R.-A. Sulfur-doped graphene quantum dot-based paper sensor for highly sensitive and selective detection of 4-nitrophenol in contaminated water and wastewater. *RSC Adv.* **2019**, *9*, 26588–26597.
188. Wang, Y.; Liu, A.; Han, Y.; Li, T. Sensors based on conductive polymers and their composites: A review. *Polym. Int.* **2020**, *69*, 7–17. [[CrossRef](#)]
189. Hathoot, A.A.; Yousef, U.S.; Shatla, A.S.; Abdel-Azzem, M. Voltammetric simultaneous determination of glucose, ascorbic acid and dopamine on glassy carbon electrode modified by NiNPs@poly 1,5-diaminonaphthalene. *Electrochim. Acta* **2012**, *85*, 531–537. [[CrossRef](#)]
190. Abdelwahab, A.A.; Lee, H.-M.; Shim, Y.-B. Selective determination of dopamine with a cibacron blue/poly-1,5-diaminonaphthalene composite film. *Anal. Chim. Acta* **2009**, *650*, 247–253. [[CrossRef](#)] [[PubMed](#)]
191. Chandra, P.; Son, N.X.; Noh, H.-B.; Goyal, R.N.; Shim, Y.-B. Investigation on the downregulation of dopamine by acetaminophen administration based on their simultaneous determination in urine. *Biosens. Bioelectron.* **2013**, *39*, 139–144. [[CrossRef](#)]
192. Kim, D.-M.; Cho, S.J.; Cho, C.-H.; Kim, K.B.; Kim, M.-Y.; Shim, Y.-B. Disposable all-solid-state pH and glucose sensors based on conductive polymer covered hierarchical AuZn oxide. *Biosens. Bioelectron.* **2016**, *79*, 165–172. [[CrossRef](#)] [[PubMed](#)]
193. Abdelwahab, A.A.; Shim, Y.-B. Nonenzymatic H₂O₂ sensing based on silver nanoparticles capped polyterthiophene/MWCNT nanocomposite. *Sens. Actuators B* **2014**, *201*, 51–58. [[CrossRef](#)]
194. Won, M.-S.; Yoon, J.-H.; Shim, Y.-B. Determination of selenium with a poly(1,8-diamino-naphthalene)-modified electrode. *Electroanalysis* **2005**, *17*, 1952–1958. [[CrossRef](#)]
195. Pallela, R.; Chandra, P.; Noh, H.-B.; Shim, Y.-B. An amperometric nanobiosensor using a biocompatible conjugate for early detection of metastatic cancer cells in biological fluid. *Biosens. Bioelectron.* **2016**, *85*, 883–890. [[CrossRef](#)]
196. Sadrolhosseini, A.R.; Habibi, M.; Soleimani, H.; Hamidon, M.N.; Fen, Y.W.; Lim, H.N. Surface plasmon resonance sensor to detect n-hexane in palm kernel oil using polypyrrole nanoparticles reduced graphene oxide layer. *J. Sensors* **2021**, *2021*, 1–13. [[CrossRef](#)]
197. Ozdokur, K.V.; Pelit, L.; Ertas, H.; Timur, S.; Ertas, F.N. Head space voltammetry: A novel voltammetric method for volatile organics and a case study for phenol. *Talanta* **2012**, *98*, 34–39. [[CrossRef](#)]
198. Besombes, J.L.; Cosnier, S.; Labbé, P.; Reverdy, G. Determination of phenol and chlorinated phenolic compounds based on a PPO-bioelectrode and its inhibition. *Anal. Lett.* **1995**, *28*, 405–424. [[CrossRef](#)]
199. Cosnier, S.; Popescu, I.C. Poly(amphiphilic pyrrole)-tyrosinase-peroxidase electrode for amplified flow injection-amperometric detection of phenol. *Anal. Chim. Acta* **1996**, *319*, 145–151. [[CrossRef](#)]
200. Cosnier, S.; Fombon, J.-J.; Labbe, P.; Limosin, D. Development of a PPO-poly(amphiphilic pyrrole) electrode for on site monitoring of phenol in aqueous effluents. *Sens. Actuators B* **1999**, *59*, 134–139. [[CrossRef](#)]
201. Mailley, P.; Cummings, E.A.; Mailley, S.C.; Eggins, B.R.; McAdams, E.; Cosnier, S. Composite carbon paste biosensor for phenolic derivatives based on in situ electrogenerated. *Anal. Chem.* **2003**, *75*, 5422–5428. [[CrossRef](#)]
202. Cosnier, S.; Innocent, C. A new strategy for the construction of a tyrosinase-based amperometric phenol and o-diphenol sensor. *Bioelectrochem. Bioenerg.* **1993**, *31*, 147–160. [[CrossRef](#)]
203. Tingry, S.; Innocent, C.; Touil, S.; Deratani, A.; Seta, P. Carbon paste biosensor for phenol detection of impregnated tissue: Modification of selectivity by using β -cyclodextrin-containing PVA membrane. *Mater. Sci. Eng. C* **2006**, *26*, 222–226. [[CrossRef](#)]
204. Li, H.; Hu, X.; Zhu, H.; Zang, Y.; Xue, H. Amperometric phenol biosensor based on a new immobilization matrix: Polypyrrole nanotubes derived from methyl orange as dopant. *Int. J. Electrochem. Sci.* **2017**, *12*, 6714–6728. [[CrossRef](#)]
205. Lu, W.; Wallace, G.G.; Imisides, M.D. Development of conducting polymer modified electrodes for the detection of phenol. *Electroanalysis* **2002**, *14*, 325–332. [[CrossRef](#)]
206. Stanca, S.E.; Popescu, I.C. Phenols monitoring and Hill coefficient evaluation using tyrosinase-based amperometric biosensors. *Bioelectrochemistry* **2004**, *64*, 47–52. [[CrossRef](#)] [[PubMed](#)]
207. Ozoner, S.K.; Kilic, M.S.; Erhan, E. Modified poly(pyrrole) film based biosensors for phenol detection. *Int. J. Chem. Mol. Nucl. Mater. Metall. Eng.* **2015**, *13*, 1173–1176.
208. Rajesh; Takashima, W.; Kaneto, K. Amperometric tyrosinase based biosensor using an electropolymerized PTS-doped polypyrrole film as an entrapment support. *React. Funct. Polym.* **2004**, *59*, 163–169. [[CrossRef](#)]
209. Rajesh; Takashima, W.; Kaneto, K. Amperometric phenol biosensor based on covalent immobilization of tyrosinase onto an electrochemically prepared novel copolymer poly(N-3-aminopropyl pyrrole-co-pyrrole) film. *Sens. Actuators B* **2004**, *102*, 271–277. [[CrossRef](#)]
210. Rajesh; Kaneto, K. A new tyrosinase biosensor based on covalent immobilization of enzyme on N-(3-aminopropyl) pyrrole polymer film. *Curr. Appl. Phys.* **2005**, *5*, 178–183. [[CrossRef](#)]

211. Rajesh; Pandey, S.S.; Takashima, W.; Kaneto, K. Development of an amperometric biosensor based on a redox-mediator-doped polypyrrole film. *J. Appl. Polym. Sci.* **2004**, *93*, 927–933. [[CrossRef](#)]
212. Rajesh; Pandey, S.S.; Takashima, W.; Kaneto, K. Simultaneous co-immobilization of enzyme and a redox mediator in polypyrrole film for the fabrication of an amperometric phenol biosensor. *Curr. Appl. Phys.* **2005**, *5*, 184–188. [[CrossRef](#)]
213. Njagi, J.; Andreescu, S. Stable enzyme biosensors based on chemically synthesized Au-polypyrrole nanocomposites. *Biosens. Bioelectron.* **2007**, *23*, 168–175. [[CrossRef](#)] [[PubMed](#)]
214. Daoa, Y.; Thanachayanont, C.; Prichanont, S. Glassy carbon electrode with decorated gold nanoparticles for horseradish peroxidase/polypyrrole nanorod biosensor. *Sensors Mater.* **2016**, *28*, 1–11.
215. Sulak, M.T.; Erhan, E.; Keskinler, B. Electrochemical phenol biosensor configurations based on nanobiocomposites. *Sensors Mater.* **2012**, *24*, 141–152.
216. Ozoner, S.K.; Keskinler, B.; Erhan, E. An amperometric biosensor based on multiwalled carbon nanotube-poly(pyrrole)-horseradish peroxidase nanobiocomposite film for determination of phenol derivatives. *Talanta* **2008**, *76*, 1147–1152.
217. Ozoner, S.K.; Yilmaz, F.; Celik, A.; Keskinler, B.; Erhan, E. A novel poly(glycine methacrylate-co-3-thienylmethyl methacrylate)-polypyrrole-carbon nanotube-horseradish peroxidase composite film electrode for the detection of phenolic compounds. *Curr. Appl. Phys.* **2011**, *11*, 402–408. [[CrossRef](#)]
218. Sulak, M.T.; Erhan, E.; Keskinler, B. Amperometric phenol biosensor based on horseradish peroxidase entrapped PVF and PPY composite film coated GC electrode. *Appl. Biochem. Biotechnol.* **2010**, *160*, 856–867. [[CrossRef](#)]
219. Dursun, F.; Ozoner, S.K.; Demirci, A.; Gorur, M.; Yilmaz, F.; Erhan, E. Vinylferrocene copolymers based biosensors for phenol derivatives. *J. Chem. Tech. Biotechnol.* **2012**, *87*, 95–104. [[CrossRef](#)]
220. Arslan, H.; Arslan, F. Preparation of a polypyrrole-polyvinylsulphonate composite film biosensor for determination of phenol based on entrapment of polyphenol oxidase. *Artif. Cells, Blood Substitutes, Biotechnol.* **2011**, *39*, 341–345. [[CrossRef](#)]
221. Arulraj, A.D.; Vijayan, M.; Vasantha, V.S. Highly selective and sensitive simple sensor based on electrochemically treated nano polypyrrole-sodium dodecyl sulphate film for the detection of para-nitrophenol. *Anal. Chim. Acta* **2015**, *899*, 66–74. [[CrossRef](#)]
222. Seo, H.-K.; Ameen, S.; Akhtar, M.S.; Shin, H.S. Structural, morphological and sensing properties of layered polyaniline nanosheets towards hazardous phenol chemical. *Talanta* **2013**, *104*, 219–227. [[CrossRef](#)] [[PubMed](#)]
223. Timur, S.; Pazarlioglu, N.; Pilloton, R.; Telefoncu, A. Thick film sensors based on laccases from different sources immobilized in polyaniline matrix. *Sens. Actuators B* **2004**, *97*, 132–136. [[CrossRef](#)]
224. Kushwah, B.S.; Upadhyaya, S.C.; Shukla, S.; Sikarwar, A.S.; Sengar, R.M.S.; Bhadauria, S. Performance of nanopolyaniline-fungal enzyme based biosensor for water pollution. *Adv. Mat. Lett.* **2011**, *2*, 43–51. [[CrossRef](#)]
225. Li, X.; Sun, C. Bioelectrochemical response of the polyaniline tyrosinase electrode to phenol. *J. Anal. Chem.* **2005**, *60*, 1073–1077. [[CrossRef](#)]
226. Xue, H.; Shen, Z. A highly stable biosensor for phenols prepared by immobilizing polyphenol oxidase into polyaniline-polyacrylonitrile composite matrix. *Talanta* **2002**, *57*, 289–295. [[CrossRef](#)]
227. Zhang, J.; Lei, J.; Liu, Y.; Zhao, J.; Ju, H. Highly sensitive amperometric biosensors for phenols based on polyaniline-ionic liquid-carbon nanofiber composite. *Biosens. Bioelectron.* **2009**, *24*, 1858–1863. [[CrossRef](#)]
228. Arslan, H.; Senarslan, D.; Cevrimli, B.S.; Zengin, H.; Uzun, D.; Arslan, F. Preparation of carbon paste electrode containing polyaniline-activated carbon composite for amperometric detection of phenol. *Bulg. Chem. Commun.* **2018**, *50*, 16–20.
229. Guo, L.; Du, H.; Zhao, H.; Li, J. Amplified electrochemical response of phenol by oxygenation of tyrosinase coupling with electrochemical-chemical-chemical redox cycle. *Electroanalysis* **2019**, *31*, 1728–1735. [[CrossRef](#)]
230. Roy, A.C.; Nisha, V.S.; Dhand, C.; Ali, M.A.; Malhotra, B.D. Molecularly imprinted polyaniline-polyvinyl sulphonic acid composite based sensor for para-nitrophenol detection. *Anal. Chim. Acta* **2013**, *777*, 63–71. [[CrossRef](#)]
231. Jovic, A.; Dordevic, A.; Cebela, M.; Simatovic, I.S.; Hercigonja, R.; Sljukic, B. Composite zeolite/carbonized polyaniline electrodes for p-nitrophenol sensing. *J. Electroanal. Chem.* **2016**, *778*, 137–147. [[CrossRef](#)]
232. Klink, M.J.; Iwuoha, E.I.; Ebenso, E.E. The electro-catalytic and redox-mediator effects of nanostructured PDMA-PSA modified-electrodes as phenol derivative sensors. *Int. J. Electrochem. Sci.* **2011**, *6*, 2429–2442.
233. Vedrine, C.; Fabiano, S.; Tran-Minh, C. Amperometric tyrosinase based biosensor using an electrogenerated polythiophene film as an entrapment support. *Talanta* **2003**, *59*, 535–544. [[CrossRef](#)]
234. Heras, M.A.; Lupu, S.; Pigani, L.; Pirvu, C.; Seeber, R.; Terzi, F.; Zanardi, C. A poly(3,4-ethylenedioxythiophene)-poly(styrene sulphonate) composite electrode coating in the electrooxidation of phenol. *Electrochim. Acta* **2005**, *50*, 1685–1691. [[CrossRef](#)]
235. Hryniewicz, B.M.; Orth, E.S.; Vidotti, M. Enzymeless PEDOT-based electrochemical sensor for the detection of nitrophenols and organophosphates. *Sens. Actuators B* **2017**, *257*, 570–578. [[CrossRef](#)]
236. Negash, N.; Alemu, H.; Tessema, M. Determination of phenol and chlorophenols at single-wall carbon nanotubes/poly(3,4-ethylenedioxythiophene) modified glassy carbon electrode using flow injection amperometry. *Anal. Chem.* **2014**, *2014*, 1–10. [[CrossRef](#)]
237. Negash, N.; Alemu, H.; Tessema, M. Electrochemical characterization and determination of phenol and chlorophenols by voltammetry at single wall carbon nanotube/poly(3,4-ethylenedioxythiophene) modified screen printed carbon electrode. *Int. Sch. Res. Not.* **2015**, *2015*, 1–11. [[CrossRef](#)] [[PubMed](#)]
238. Ann Maria, C.G.; Akshaya, K.B.; Rison, S.; Varghese, A.; George, L. Molecularly imprinted PEDOT on carbon fiber paper electrode for the electrochemical determination of 2,4-dichlorophenol. *Synth. Met.* **2020**, *261*, 116309. [[CrossRef](#)]

239. Bagheri, H.; Mohammadi, A. Pyrrole-based conductive polymer as the solid-phase extraction medium for the preconcentration of environmental pollutants in water samples followed by gas chromatography with flame ionization and mass spectrometry detection. *J. Chromatogr. A* **2003**, *1015*, 23–30. [[CrossRef](#)]
240. Bagheri, H.; Mohammadi, A.; Salemi, A. On-line trace enrichment of phenolic compounds from water using a pyrrole-based polymer as the solid-phase extraction sorbent coupled with high-performance liquid chromatography. *Anal. Chim. Acta* **2004**, *513*, 445–449. [[CrossRef](#)]
241. Tahmasebi, E.; Yamini, Y.; Seidi, S.; Rezazadeh, M. Extraction of three nitrophenols using polypyrrole-coated magnetic nanoparticles based on anion exchange process. *J. Chromatogr. A* **2013**, *1314*, 15–23. [[CrossRef](#)]
242. Abolghasemi, M.M.; Parastari, S.; Yousefi, V. Polypyrrole-montmorillonite nanocomposite as sorbent for solid-phase microextraction of phenolic compounds in water. *J. Sep. Sci.* **2014**, *37*, 3526–3532. [[CrossRef](#)] [[PubMed](#)]
243. Bagheri, H.; Saraji, M. New polymeric sorbent for the solid-phase extraction of chlorophenols from water samples followed by gas chromatography-electron-capture detection. *J. Chromatogr. A* **2001**, *910*, 87–93. [[CrossRef](#)]
244. Bagheri, H.; Saraji, M. Conductive polymers as new media for solid-phase extraction: Isolation of chlorophenols from water sample. *J. Chromatogr. A* **2003**, *986*, 111–119. [[CrossRef](#)]
245. Bagheri, H.; Mir, A.; Babanezhad, E. An electropolymerized aniline-based fiber coating for solid phase microextraction of phenols from water. *Anal. Chim. Acta* **2005**, *532*, 89–95. [[CrossRef](#)]
246. Mousavi, M.; Noroozian, E.; Jalali-Heravi, M.; Mollahosseini, A. Optimization of solid-phase microextraction of volatile phenols in water by a polyaniline-coated Pt-fiber using experimental design. *Anal. Chim. Acta* **2007**, *581*, 71–77. [[CrossRef](#)]
247. Du, W.; Zhao, F.; Zeng, B. Novel multiwalled carbon nanotubes–polyaniline composite film coated platinum wire for headspace solid-phase microextraction and gas chromatographic determination of phenolic compounds. *J. Chromatogr. A* **2009**, *1216*, 3751–3757. [[CrossRef](#)]
248. Meng, J.; Shi, C.; Wei, B.; Yu, W.; Deng, C.; Zhang, X. Preparation of Fe₃O₄@C@PANI magnetic microspheres for the extraction and analysis of phenolic compounds in water samples by gas chromatography-mass spectrometry. *J. Chromatogr. A* **2011**, *1218*, 2841–2847. [[CrossRef](#)] [[PubMed](#)]
249. Tafazoli, Z.; Azar, P.A.; Tehrani, M.S.; Husain, S.W. Facile preparation of multifunctional carbon nanotube/magnetite/polyaniline nanocomposite offering a strong option for efficient solid-phase microextraction coupled with GC-MS for the analysis of phenolic compounds. *J. Sep. Sci.* **2018**, *41*, 2736–2742. [[CrossRef](#)]
250. Zhang, Y.; Wu, L.; Lei, W.; Xia, X.; Xia, M.; Hao, Q. Electrochemical determination of 4-nitrophenol at polycarbazole/N-doped graphene modified glassy carbon electrode. *Electrochim. Acta* **2014**, *146*, 568–576. [[CrossRef](#)]
251. Saadati, F.; Ghahramani, F.; Shayani-jam, H.; Piri, F.; Yafian, M.R. Synthesis and characterization of nanostructure molecularly imprinted polyaniline/graphene oxide composite as highly selective electrochemical sensor for detection of p-nitrophenol. *J. Taiwan Inst. Chem. Eng.* **2018**, *86*, 213–221. [[CrossRef](#)]
252. Hashemi, S.A.; Mousavi, S.M.; Bahrani, S.; Ramakrishna, S. Integrated polyaniline with graphene oxide-iron tungsten nitride nanoflakes as ultrasensitive electrochemical sensor for precise detection of 4-nitrophenol within aquatic media. *J. Electroanal. Chem.* **2020**, *873*, 114406. [[CrossRef](#)]
253. Zhu, G.; Tang, Q.; Dou, J.; Li, X.; Yang, J.; Xu, R.; Liu, J. Partially reduced graphene oxide sheet-covered polyaniline nanotubes for the simultaneous determination of bisphenol A and phenol. *J. Electrochem. Soc.* **2019**, *166*, 1661–1668. [[CrossRef](#)]
254. Peleyeju, M.G.; Idris, A.O.; Umukoro, E.H.; Babalola, J.O.; Arotiba, O.A. Electrochemical detection of 2,4-dichlorophenol on a ternary composite electrode of diamond, graphene, and polyaniline. *ChemElectroChem* **2017**, *3*, 1074–1080. [[CrossRef](#)]
255. Khan, A.; Khan, A.A.P.; Rahman, M.M.; Asiri, A.M.; Inamuddin; Alamry, K.A.; Hameed, S.A. Preparation and characterization of PANI@G/CWO nanocomposite for enhanced 2-nitrophenol sensing. *Appl. Surf. Sci.* **2018**, *433*, 696–704. [[CrossRef](#)]
256. Zou, J.; Song, X.; Ji, J.; Xu, W.; Chen, J.; Jiang, Y.; Wang, Y.; Chen, X. Polypyrrole/graphene composite-coated fiber for the solid-phase microextraction of phenols. *J. Sep. Sci.* **2011**, *34*, 2765–2772. [[CrossRef](#)] [[PubMed](#)]
257. Jiang, Y.; Gu, Y.; Nie, G.; Chi, M.; Yang, Z.; Wang, C.; Wei, Y.; Lu, X. Synthesis of RGO/Cu₈S₅/PPy composite nanosheets with enhanced peroxidase-like activity for sensitive colorimetric detection of H₂O₂ and phenol. *Part. Part. Syst. Charact.* **2017**, *34*, 1600233. [[CrossRef](#)]
258. Talarico, D.; Arduini, F.; Constantino, A.; Del Carlo, M.; Compagnone, D.; Moscone, D.; Palleschi, G. Carbon black as successful screen-printed electrode modifier for phenolic compound detection. *Electrochem. Commun.* **2015**, *60*, 78–82. [[CrossRef](#)]
259. Chen, K.; Zhang, Z.-L.; Liang, Y.-M.; Liu, W. A graphene-based electrochemical sensor for rapid determination of phenols in water. *Sensors* **2013**, *13*, 6204–6216. [[CrossRef](#)] [[PubMed](#)]
260. Anas, N.A.A.; Fen, Y.W.; Omar, N.A.S.; Daniyal, W.M.E.M.M.; Ramdzan, N.S.M.; Saleviter, S. Development of graphene quantum dots-based optical sensor for toxic metal ion detection. *Sensors* **2019**, *19*, 3850. [[CrossRef](#)] [[PubMed](#)]